

On the Unbounded External Archive and Population Size in Preference-based Evolutionary Multi-objective Optimization Using a Reference Point

Ryoji Tanabe

Yokohama National University
Yokohama, Kanagawa, Japan
rt.ryoji.tanabe@gmail.com

ABSTRACT

Although the population size is an important parameter in evolutionary multi-objective optimization (EMO), little is known about its influence on preference-based EMO (PBEMO). The effectiveness of an unbounded external archive (UA) in PBEMO is also poorly understood, where the UA maintains all non-dominated solutions found so far. In addition, existing methods for postprocessing the UA cannot handle the decision maker's preference information. In this context, first, this paper proposes a preference-based postprocessing method for selecting representative solutions from the UA. Then, we investigate the influence of the UA and population size on the performance of PBEMO algorithms. Our results show that the performance of PBEMO algorithms (e.g., R-NSGA-II) can be significantly improved by using the UA and the proposed method. We demonstrate that a smaller population size than commonly used is effective in most PBEMO algorithms for a small budget of function evaluations, even for many objectives. We found that the size of the region of interest is a less important factor in selecting the population size of the PBEMO algorithms on real-world problems.

CCS CONCEPTS

• **Mathematics of computing** → **Evolutionary algorithms.**

KEYWORDS

Preference-based evolutionary multi-objective optimization, unbounded external archive, population size, benchmarking

ACM Reference Format:

Ryoji Tanabe. 2023. On the Unbounded External Archive and Population Size in Preference-based Evolutionary Multi-objective Optimization Using a Reference Point. In *Genetic and Evolutionary Computation Conference (GECCO '23)*, July 15–19, 2023, Lisbon, Portugal. ACM, New York, NY, USA, 24 pages. <https://doi.org/10.1145/3583131.3590511>

1 INTRODUCTION

General context. The ultimate goal of multi-objective optimization involves finding a Pareto optimal solution preferred by a decision maker (DM) [33]. Evolutionary multi-objective optimization (EMO) is helpful for finding a solution set that approximates the Pareto

front (PF) in the objective space [15]. Representative EMO algorithms include NSGA-II [16], IBEA [52], and MOEA/D [51]. The solution set found by an EMO algorithm is generally used for an *a posteriori* decision-making, where the DM selects a single solution from the solution set. The *a posteriori* decision-making is practical when any preference information from the DM is unavailable.

When the DM's preference information is available *a priori*, it can be incorporated into EMO algorithms [38]. A preference-based EMO (PBEMO) algorithm [4, 12] aims to approximate the region of interest (ROI), which is a subregion of the PF defined by the DM's preference information [40]. From the perspective of optimization algorithms, approximating a subregion of the PF is generally easier than approximating the whole one, especially for many objectives. From the perspective of the DM, she/he can examine only a set of her/his potentially preferred solutions, rather than a set of irrelevant solutions. That is, using the DM's preference information can reduce her/his workload.

Although a number of ways of expressing the preference have been proposed in the literature [4], using a reference point [50] is one of the most popular approaches [1, 30]. The reference point consists of objective values desired by the DM. Compared to other approaches, the reference point-based approach is intuitive and thus relatively easy for the DM to express her/his preference information. Throughout this paper, we focus only on PBEMO using the reference point. Representative PBEMO algorithms include R-NSGA-II [19], PBEA [49], and MOEA/D-NUMS [28]. These PBEMO algorithms were designed to approximate the ROI.

The population size μ is one of the most important parameters in evolutionary algorithms. Some previous studies investigated the influence of the population size on the performance of conventional EMO algorithms (e.g., NSGA-II, not R-NSGA-II). For example, Dymond et al. [22] showed that the best population size of NSGA-II and SPEA2 [53] depends on a budget of function evaluations. Brockhoff et al. [10] showed that NSGA-II with a large population size performs poorly at an early stage of the search but performs well at a later stage. Ishibuchi et al. [26] showed that the best population size depends on the type of EMO algorithm. Some previous studies (e.g., [5, 39]) analyzed the influence of the population size on EMO algorithms by using an automatic algorithm configurator.

With some exceptions (e.g., PESA [14] and ϵ -MOEA [18]), EMO algorithms maintain only μ solutions in the population. Thus, as pointed out in [8], most EMO algorithms are likely to discard solutions in which the DM may be interested. As demonstrated in previous studies (e.g., [8, 32]), this issue can be easily addressed by using an unbounded external archive (UA), which maintains

GECCO '23, July 15–19, 2023, Lisbon, Portugal

© 2023 Copyright held by the owner/author(s). Publication rights licensed to ACM. This is the author's version of the work. It is posted here for your personal use. Not for redistribution. The definitive Version of Record was published in *Genetic and Evolutionary Computation Conference (GECCO '23)*, July 15–19, 2023, Lisbon, Portugal, <https://doi.org/10.1145/3583131.3590511>.

all non-dominated solutions found so far. The UA can be incorporated into any EMO algorithm in a plug-in manner. Since the UA works independently of EMO algorithms, the UA does not influence their search behavior. An EMO algorithm with the UA generally outperforms the one without the UA [5, 32, 46].

One disadvantage of using the UA is that its size can be very large, especially for many-objective optimization. In practice, the DM does not want to examine so many solutions [51]. To address this issue, some methods for postprocessing the UA have been proposed (e.g., [8, 45]). One of the simplest methods is the distance-based subset selection method [45], which aims to select a subset of uniformly distributed solutions in the objective space from the UA.

Motivation. Unlike the situation in EMO, little is known about the influence of the population size μ on the performance of PBEMO algorithms. The population size μ in PBEMO has also not been standardized in the literature. Table 1 shows the number of objectives m , population size μ , and maximum number of function evaluations max_evals used in previous studies. For the sake of reference, Table 1 shows the setup in the previous study [16] that proposed NSGA-II. As shown in Table 1, the four previous studies set μ and max_evals to different values. PBEMO algorithms approximate the ROI rather than the whole PF. Thus, it is *intuitively* expected that PBEMO requires only small values of μ and max_evals compared to EMO. However, except for [49], the previous studies used relatively larger values of μ and max_evals compared to [16].

In addition, the UA has received little attention in the field of PBEMO. Except for the earliest study [23], most previous studies discussed the performance of PBEMO algorithms based only on the quality of the final population. The reason for not using the UA may be that existing methods for postprocessing the UA are unlikely to work well for PBEMO. This is because existing postprocessing methods cannot handle the DM's preference information.

Contributions. Motivated by the above discussion, first, we propose a preference-based postprocessing method for selecting representative solutions from the UA. Then, we analyze the behavior of PBEMO algorithms with different population sizes. Through an analysis, we address the following three research questions:

- RQ1: Can the performance of PBEMO algorithms be improved by using the UA? Should a postprocessing method of the UA handle the DM's preference information?
- RQ2: How do the number of objectives and a budget of function evaluations influence the best population size? Is the population size used in previous studies reasonable?
- RQ3: Is the size of the ROI a key factor in selecting the population size of PBEMO algorithms?

Outline. Section 2 gives some preliminaries. Section 3 introduces the proposed postprocessing method. Section 4 describes our experimental setup. Section 5 shows the analysis results to answer the three research questions. Section 6 concludes this paper.

Supplementary file. Figure S.* and Table S.* indicate a figure and a table in the supplementary file, respectively.

Code availability. The implementation of the proposed postprocessing method is available at <https://github.com/ryojitanabe/prefpp>.

Table 1: m , μ , and max_evals used in previous studies.

Ref.	m	μ	max_evals
NSGA-II [16]	2, 5	100	5×10^4
R-NSGA-II [19]	2, 3, 5, 10	100–500	$5 \times 10^4 - 2.5 \times 10^5$
PBEA [49]	2, 5	20–200	$2 \times 10^3, 2 \times 10^4$
R-MEAD2 [36]	4, ..., 10	200–350	$6 \times 10^4, 9 \times 10^4, 1.05 \times 10^5$
NUMS [28]	2, 3, 5, 8, 10	100–660	$4 \times 10^4 - 1.188 \times 10^6$

2 PRELIMINARIES

2.1 Multi-objective optimization

This paper considers minimization problems. Multi-objective optimization aims to find a solution $\mathbf{x} \in \mathbb{X}$ that minimizes an objective function vector $\mathbf{f} : \mathbb{X} \rightarrow \mathbb{R}^m$, where $\mathbb{X} \subseteq \mathbb{R}^n$ is the feasible solution space, and \mathbb{R}^m is the objective space. Thus, n is the dimension of the solution space, and m is the dimension of the objective space.

A solution \mathbf{x}_1 is said to dominate \mathbf{x}_2 if $f_i(\mathbf{x}_1) \leq f_i(\mathbf{x}_2)$ for all $i \in \{1, \dots, m\}$ and $f_i(\mathbf{x}_1) < f_i(\mathbf{x}_2)$ for at least one index i . We denote $\mathbf{x}_1 < \mathbf{x}_2$ when \mathbf{x}_1 dominates \mathbf{x}_2 . In addition, \mathbf{x}_1 is said to weakly dominate \mathbf{x}_2 if $f_i(\mathbf{x}_1) \leq f_i(\mathbf{x}_2)$ for all $i \in \{1, \dots, m\}$. A solution \mathbf{x}^* is a Pareto optimal solution if \mathbf{x}^* is not dominated by any solution in \mathbb{X} . The set of all Pareto optimal solutions in \mathbb{X} is called the Pareto optimal solution set $\mathcal{X}^* = \{\mathbf{x}^* \in \mathbb{X} \mid \nexists \mathbf{x} \in \mathbb{X} \text{ s.t. } \mathbf{x} < \mathbf{x}^*\}$. The image of the Pareto optimal solution set in \mathbb{R}^m is also called the PF $\mathbf{f}(\mathcal{X}^*)$. The ideal and nadir points consist of the minimum and maximum values of the PF for m objective functions, respectively.

2.2 Preference-based multi-objective optimization using the reference point

Preference-based multi-objective optimization using the reference point \mathbf{z} involves finding a set of solutions in the ROI in the objective space. Here, the ROI is a subregion of the PF defined by \mathbf{z} . While EMO aims to approximate the PF, PBEMO aims to approximate the ROI. It is expected that approximating the ROI is relatively easier than approximating the PF. In addition, most solutions in the ROI are potentially preferred by the DM. Thus, the DM's workload is relatively low in this case.

This paper considers the ROI based on the closest Pareto optimal objective vector $\mathbf{f}(\mathbf{x}^{c*})$ to the reference point \mathbf{z} in terms of the Euclidean distance. This ROI is called the ROI-C in [48]. Although three ROIs were reviewed in [48], this ROI is the most intuitive ROI. Mathematically, this ROI is defined as follows:

$$\text{ROI} = \{\mathbf{f}(\mathbf{x}^*) \in \mathbf{f}(\mathcal{X}^*) \mid \text{distance}(\mathbf{f}(\mathbf{x}^*), \mathbf{f}(\mathbf{x}^{c*})) < r\}, \quad (1)$$

$$\mathbf{x}^{c*} = \underset{\mathbf{x}^* \in \mathcal{X}^*}{\text{argmin}} \{\text{distance}(\mathbf{f}(\mathbf{x}^*), \mathbf{z})\},$$

where $\text{distance}(\cdot, \cdot)$ returns the Euclidean distance between two inputs. In equation (1), r determines the radius of the ROI.

Figure 1 shows an example of the ROI on the bi-objective DTLZ1 problem, where the shape of the PF is linear. As shown in Figure 1, the ROI is a set of objective vectors of Pareto optimal solutions in a hypersphere of a radius r centered at $\mathbf{f}(\mathbf{x}^{c*})$. As discussed in [48], some PBEMO algorithms (e.g., R-NSGA-II [19] and R-MEAD2 [36]) were implicitly designed to approximate this ROI.

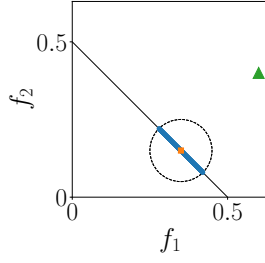


Figure 1: Example of the ROI on DTLZ1 with $m = 2$, where \blacktriangle is the reference point $\mathbf{z} = (0.6, 0.4)^\top$, \blacksquare is the objective vector of the closet Pareto optimal solution $\mathbf{f}(\mathbf{x}^{c*})$ to \mathbf{z} , and $r = 0.1$. A set of the objective vectors of Pareto optimal solutions \bullet in the dotted circle is the ROI.

2.3 Quality indicators for PBEMO

Quality indicators evaluate the quality of a set of objective vectors [31, 55]. Quality indicators play a crucial role in benchmarking EMO algorithms. Representative quality indicators include the hypervolume (HV) [54], additive ϵ -indicator ($I_{\epsilon+}$) [55], and inverted generational distance (IGD) [13]. For example, the IGD value of a solution set \mathcal{X} is calculated as follows:

$$\text{IGD}(\mathcal{X}) = \frac{1}{|\mathcal{S}|} \left(\sum_{\mathbf{s} \in \mathcal{S}} \min_{\mathbf{x} \in \mathcal{X}} \{ \text{distance}(\mathbf{f}(\mathbf{x}), \mathbf{s}) \} \right), \quad (2)$$

where \mathcal{S} is a set of IGD-reference points $\mathbf{s} \in \mathbb{R}^m$. It is desirable that the IGD-reference points in \mathcal{S} are uniformly distributed on the PF. In equation (2), IGD measures the average distance from each $\mathbf{s} \in \mathcal{S}$ to its nearest objective vector $\mathbf{f}(\mathbf{x})$. A small IGD value indicates a good quality of \mathcal{X} in terms of both convergence and diversity.

Since IGD is not Pareto-compliant, IGD can lead to the wrong conclusion [24, 43]. To address this issue, a weakly Pareto-compliant version of IGD (IGD^+) was proposed in [24]. IGD^+ uses the following distance measure instead the distance function in equation (2):

$$\text{distance}_{\text{IGD}^+}(\mathbf{f}(\mathbf{x}), \mathbf{s}) = \sqrt{\sum_{i=1}^m (\max\{f_i(\mathbf{x}) - s_i, 0\})^2}.$$

Conventional quality indicators (e.g., IGD) do not take into account any preference information defined by the reference point \mathbf{z} . Thus, conventional quality indicators are not suitable for benchmarking PBEMO algorithms. As discussed in [48], quality indicators for PBEMO should be able to assess $\mathbf{f}(\mathcal{X})$ from the following three aspects: *i*) the convergence to the PF, *ii*) the convergence to the reference point \mathbf{z} , and *iii*) the diversity in the ROI. Quality indicators for PBEMO should also be able to evaluate the quality of $\mathbf{f}(\mathcal{X})$ even when it is outside the ROI.

Although some quality indicators for benchmarking PBEMO algorithms (e.g., [2, 29, 35]) have been proposed, IGD-C [36] was recommended in [48]. IGD-C was implicitly designed for the ROI in equation (1) and can address the three aspects *i* – *iii*). The IGD-C value of \mathcal{X} is calculated by equation (2) using $\mathcal{S}' \subseteq \mathcal{S}$ instead of \mathcal{S} . While the IGD-reference points in \mathcal{S} are distributed on the PF, those in \mathcal{S}' are distributed only on the ROI. In the example in Figure 1, \mathcal{S}' can be only in the dotted circle. To select \mathcal{S}' from \mathcal{S} , first, the closest point \mathbf{s}^c to \mathbf{z} is selected from \mathcal{S} , i.e., $\mathbf{s}^c = \underset{\mathbf{s} \in \mathcal{S}}{\text{argmin}} \{ \text{distance}(\mathbf{s}, \mathbf{z}) \}$.

Then, \mathcal{S}' is a set of all points in the region of a hypersphere of radius r centered at \mathbf{s}^c , i.e., $\mathcal{S}' = \{ \mathbf{s} \in \mathcal{S} \mid \text{distance}(\mathbf{s}, \mathbf{s}^c) < r \}$.

2.4 Preference-based EMO algorithms

As reviewed in [4], some PBEMO algorithms have been proposed in the literature. As in [30], this paper focuses on the following six PBEMO algorithms: R-NSGA-II [19], r-NSGA-II [41], g-NSGA-II [37], PBEA [49], R-MEAD2 [36], and MOEA/D-NUMS [28]. Note that none of the six PBEMO algorithms use the UA.

R-NSGA-II, r-NSGA-II, and g-NSGA-II are extended versions of NSGA-II [16] for preference-based multi-objective optimization. R-NSGA-II measures the distance to the reference point \mathbf{z} , instead of the crowding distance. Thus, R-NSGA-II prefers non-dominated individuals close to \mathbf{z} . R-NSGA-II also performs ϵ -clearing to maintain the diversity of the population. r-NSGA-II uses the r-dominance relation instead of the Pareto dominance relation. The r-dominance relation prefers individuals close to \mathbf{z} , and the size of its preferred region is determined by a parameter $\delta \in [0, 1]$. Similarly, g-NSGA-II uses the g-dominance relation instead of the Pareto dominance relation. The g-dominance relation prefers non-dominated individuals in a region, which is the set of all objective vectors in \mathbb{R}^m that dominate \mathbf{z} or are dominated by \mathbf{z} .

PBEA [49] is an extended version of IBEA [52] by replacing the binary additive ϵ -indicator ($I_{\epsilon+}$) with a preference-based one. The indicator in PBEA handles the DM's preference information by using an augmented achievement scalarizing function [34].

R-MEAD2 and MOEA/D-NUMS are scalarizing function-based PBEMO algorithms using a set of μ weight vectors $\mathcal{W} = \{\mathbf{w}_i\}_{i=1}^\mu$. Although R-MEAD2 is similar to MOEA/D [51], R-MEAD2 adaptively adjusts the μ weight vectors so that the μ individuals move toward \mathbf{z} in the objective space. The previous study [28] proposed a nonuniform mapping scheme (NUMS) that shifts the μ weight vectors toward \mathbf{z} . In contrast to R-MEAD2, NUMS adjusts the weight vectors in an offline manner. MOEA/D-NUMS [28] is an extended MOEA/D using \mathcal{W} generated by NUMS. MOEA/D-NUMS also uses an augmented achievement scalarizing function [34].

2.5 Subset selection method

As mentioned in Section 1, a postprocessing method is necessary to select k representative solutions from the UA \mathcal{A} . This is exactly the subset selection problem that aims to find a subset \mathcal{X} of size k from \mathcal{A} [3]. Since the subset selection problem is generally NP-hard [7], an inexact approach (e.g., greedy search and local search) is a reasonable first choice. However, there is a trade-off between the computational cost and the quality of a subset.

Shang et al. [45] investigated the performance of some distance-based subset selection (DSS) methods that aim to find a subset of uniformly distributed solutions in the objective space. Their results showed that an iterative DSS (IDSS) method can obtain a better subset than other methods while keeping the computational cost low. The IDSS method aims to find a subset \mathcal{X} of size k that maximizes the following uniformity level [42].

$$\text{uniformity}(\mathcal{X}) = \min_{\mathbf{x}_1 \in \mathcal{X}, \mathbf{x}_2 \in \mathcal{X} \setminus \{\mathbf{x}_1\}} \text{distance}(\mathbf{f}'(\mathbf{x}_1), \mathbf{f}'(\mathbf{x}_2)),$$

where $\mathbf{f}'(\mathbf{x})$ is the normalized objective vector of \mathbf{x} based on the maximum and minimum values of $\mathbf{f}(\mathcal{X})$.

Algorithm 1: IDSS [45]

```

1 if  $|\mathcal{A}| \leq k$  then
2   return  $\mathcal{A}$ ;
3 else
4    $\mathcal{X} \leftarrow$  Randomly select  $k$  solutions from  $\mathcal{A}$ ;
5   for  $t \in \{1, \dots, t^{\max}\}$  do
6      $\mathbf{x}^{\text{new}} \leftarrow$  Randomly select a solution from  $\mathcal{A} \setminus \mathcal{X}$ ;
7      $\mathcal{X} \leftarrow \mathcal{X} \cup \{\mathbf{x}^{\text{new}}\}$ ;
8      $\mathbf{x}^{\text{w}} \leftarrow \operatorname{argmax}_{\mathbf{x} \in \mathcal{X}} \{\text{uniformity}(\mathcal{X} \setminus \{\mathbf{x}\})\}$ ;
9      $\mathcal{X} \leftarrow \mathcal{X} \setminus \{\mathbf{x}^{\text{w}}\}$ ;
10  return  $\mathcal{X}$ ;
    
```

Algorithm 1 shows the IDSS method. \mathcal{A} is the UA that includes only non-dominated solutions. If the size of \mathcal{A} is equal to or smaller than k , Algorithm 1 returns \mathcal{A} (lines 1–2). Otherwise, \mathcal{X} is set to k solutions randomly selected from \mathcal{A} (line 4). Then, the following steps are performed t^{\max} times. First, the new solution \mathbf{x}^{new} is randomly selected from $\mathcal{A} \setminus \mathcal{X}$ (line 6), and \mathbf{x}^{new} is added to \mathcal{X} (line 7). Then, the IDSS method removes the solution \mathbf{x}^{w} with the worst contribution to the uniformity level of \mathcal{X} (lines 8–9). If t^{\max} is large enough, IDSS is likely to obtain $\mathbf{f}(\mathcal{X})$ with the uniform distribution.

3 PROPOSED POSTPROCESSING METHOD

This section introduces the proposed preference-based postprocessing method for the UA in PBEMO. Let \mathcal{A} be the UA that includes all non-dominated solutions found so far by a PBEMO algorithm. The goal here is to find a subset \mathcal{X} of size k with the uniform distribution on the ROI in the objective space. We believe that this goal addresses the three aspects *i* – *iii*) that are required for quality indicators for PBEMO (see Section 2.3). However, existing postprocessing methods (e.g., the IDSS method [45]) are unlikely to achieve this goal. This is because they were designed to find \mathcal{X} with the uniform distribution on *the whole PF* in the objective space. To address this issue, we propose the preference-based postprocessing method that can handle the DM’s preference information. Note that the proposed method is designed for the ROI defined in equation (1). Note also that the proposed method can be incorporated even into any conventional EMO algorithm.

Algorithm 2 shows the proposed method. As in Algorithm 1, if $|\mathcal{A}| \leq k$, Algorithm 2 returns \mathcal{A} (lines 1–2). Otherwise, the following steps are performed. First, the proposed method approximates the ROI, which is unknown in real-world problems. The closest solution \mathbf{x}^c to the reference point \mathbf{z} in the objective space is selected from \mathcal{A} (line 4). We denote the set of all non-dominated solutions in an m -dimensional hypersphere of radius r centered at \mathbf{x}^c in the objective space as an *approximated ROI*. Here, the approximated ROI is equivalent to the true ROI in equation (1) if $\mathcal{A} = \mathcal{X}^*$. All non-dominated solutions in the approximated ROI are set to \mathcal{X} (line 5). If the size of \mathcal{X} is exactly the same as k , Algorithm 2 returns \mathcal{X} (lines 11). Otherwise, the following two cases are considered:

- (1) the size of \mathcal{X} is less than k (lines 6–8), and
- (2) the size of \mathcal{X} is greater than k (line 9–10).

Algorithm 2: The proposed preference-based postprocessing method for PBEMO

```

1 if  $|\mathcal{A}| \leq k$  then
2   return  $\mathcal{A}$ ;
3 else
4    $\mathbf{x}^c \leftarrow \operatorname{argmin}_{\mathbf{x} \in \mathcal{A}} \{\text{distance}(\mathbf{f}(\mathbf{x}), \mathbf{z})\}$ ;
5    $\mathcal{X} \leftarrow \{\mathbf{x} \in \mathcal{A} \mid \text{distance}(\mathbf{f}(\mathbf{x}), \mathbf{f}(\mathbf{x}^c)) \leq r\}$ ;
6   while  $|\mathcal{X}| < k$  do
7      $\mathbf{x}^{c'} \leftarrow \operatorname{argmin}_{\mathbf{x} \in \mathcal{A} \setminus \mathcal{X}} \{\text{distance}(\mathbf{f}(\mathbf{x}), \mathbf{f}(\mathbf{x}^c))\}$ ;
8      $\mathcal{X} \leftarrow \mathcal{X} \cup \{\mathbf{x}^{c'}\}$ ;
9   if  $|\mathcal{X}| > k$  then
10     $\mathcal{X} \leftarrow \text{subset\_selection}(\mathcal{X}, k)$ ;
11  return  $\mathcal{X}$ ;
    
```

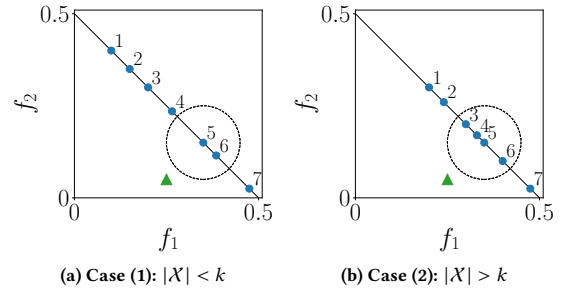


Figure 2: Examples on DTLZ1 with $m = 2$, where $|\mathcal{A}| = 7$ and $k = 3$. \blacktriangle is the reference point.

Figure 2 shows examples of the two cases, where $|\mathcal{A}| = 7$ and $k = 3$. In our preliminary results, we observed that case (1) occurs in an early stage of the search, while case (2) occurs in a later stage.

In case (1), we believe that the DM is interested in closer solutions to \mathbf{x}^c in the objective space even though they are out of the approximated ROI. Thus, it is rationale to select $k - |\mathcal{X}|$ non-dominated solutions from $\mathcal{A} \setminus \mathcal{X}$. While $|\mathcal{X}| < k$, the following steps are repeatedly performed. First, the closest solution $\mathbf{x}^{c'}$ to \mathbf{x}^c in the objective space is selected from $\mathcal{A} \setminus \mathcal{X}$ (line 7). Then, $\mathbf{x}^{c'}$ is added to \mathcal{X} (line 8). In the example of Figure 2(a), $\mathcal{X} = \{\mathbf{x}_5, \mathbf{x}_6\}$, and \mathbf{x}_5 is \mathbf{x}^c . In this case, \mathbf{x}_4 is closer to \mathbf{x}_5 than $\mathbf{x}_1, \mathbf{x}_2, \mathbf{x}_3$, and \mathbf{x}_7 in the objective space. Thus, \mathbf{x}_4 is added to \mathcal{X} .

In case (2), $|\mathcal{X}| - k$ solutions should be removed from \mathcal{X} while keeping the diversity of \mathcal{X} . Fortunately, a conventional subset selection method can be used to select k solutions from \mathcal{X} (line 10). Based on the promising results reported in [44], this paper uses the IDSS method shown in Algorithm 1. Note that IDSS cannot handle the DM’s preference information, but the objective vectors of the solutions in \mathcal{X} are already in the approximated ROI. After applying IDSS to \mathcal{X} , it is expected that the objective vectors of the k solutions in \mathcal{X} are uniformly distributed in the approximate ROI. In the example of Figure 2(b), $\mathcal{X} = \{\mathbf{x}_3, \mathbf{x}_4, \mathbf{x}_5, \mathbf{x}_6\}$, and $k = 3$. In this case, \mathbf{x}_4 is likely to be removed from \mathcal{X} after IDSS is performed.

4 EXPERIMENTAL SETUP

Here, we describe the experimental setup for our analysis. A non-dominated sorting method is required to maintain the UA. We used the ND-Tree-based update method [27], which is one of the state-of-the-art methods. We used the C++ implementation of the ND-Tree-based update method provided by the authors of [27]. As in [47], we periodically updated the archive at 100, 200, . . . , 1 000, 2 000, . . . , 50 000 function evaluations. We also implemented the proposed preference-based postprocessing method in C++, including the IDSS method [45]. Unless otherwise noted, we set the size of the subset k and the radius of the ROI r to 100 and 0.1, respectively. As in [45], we set the maximum number of iterations t^{\max} in the IDSS to 10^4 .

We used the six PBEMO algorithms described in Section 2.4. We used the source code of the PBEMO algorithms provided by the authors of [30]. We performed 31 independent runs for each PBEMO algorithm. We set the population size μ to 8, 20, 40, 100, 200, 300, 400, and 500. We set other parameters of the six PBEMO algorithms according to [30]. We investigated the effect of the population size by fixing other parameters to default values. Correlation analysis of all parameters (e.g., ϵ in R-NSGA-II) is beyond the scope of this paper. We generated the weight vector set in MOEA/D-NUMS using the source code provided by the authors of [28]. We also generated the original weight vector set using the method proposed in [6], which can generate the weight vector set of any size.

As in [2], we used the DTLZ1–DTLZ4 problems [20]. As observed in the results of EMO algorithms in [46], we believe that PBEMO algorithms require a large population size on problems with irregular PFs (e.g., DTLZ5 and DTLZ7). An investigation on problems with differently scaled objectives (e.g., SDTLZ1 [17]) remains for future work. We set the number of objectives m as follows: $m \in \{2, 3, 4, 5, 6\}$. We set the number of decision variables as in [20]. We set the reference point \mathbf{z} as follows: $\mathbf{z} = (0.6, 0.4)^\top$, $\mathbf{z} = (0.5, 0.3, 0.2)^\top$, $\mathbf{z} = (0.4, 0.3, 0.2, 0.1)^\top$, $\mathbf{z} = (0.3, 0.25, 0.2, 0.15, 0.1)^\top$, and $\mathbf{z} = (0.3, 0.2, 0.15, 0.13, 0.12, 0.1)^\top$ for $m = 2, \dots, 6$, respectively. Most reference points are achievable, but the behavior of the PBEMO algorithms (except for g-NSGA-II) is not very sensitive to the position of \mathbf{z} unless \mathbf{z} is too far from the PF [30, 48].

Although the IGD-C indicator was recommended in [48], IGD-C is not Pareto-compliant. To address this issue, we replaced the IGD calculation in IGD-C with the IGD⁺ calculation. We denote this version of IGD-C as IGD⁺-C. IGD⁺-C is more reliable than IGD-C in terms of Pareto-compliance.

5 RESULTS

This section describes our analysis results. Through experiments, Sections 5.1–5.3 aim to address the three research questions (RQ1–RQ3) described in Section 1, respectively.

5.1 On the effectiveness of the proposed postprocessing method

In this section, we consider the following three solution sets found by each PBEMO algorithm:

- **POP**: the final population of size μ ,
- **UA-IDDS**: a solution subset of size k obtained by postprocessing the UA using the IDSS method, and

- **UA-PP**: a solution subset of size k obtained by postprocessing the UA using the preference-based postprocessing (PP) method.

We focus on the results of the PBEMO algorithms with $\mu = 100$, i.e., $\mu = k$. Most previous studies evaluated the performance of a PBEMO algorithm based on its POP. In contrast, this is the first study to evaluate the performance of a PBEMO algorithm based on its UA-IDDS and UA-PP.

5.1.1 Distributions of objective vectors. Figure 3 shows distributions of the objective vectors of the solutions in POP, UA-IDDS, and UA-PP on the bi-objective DTLZ2 problem. Figure 3 shows the result of a single run for each PBEMO algorithm. Figures S.1–S.3 show the results on DTLZ1, DTLZ3, and DTLZ4 problems, respectively.

Results of POP. As shown in Figures 3(a), (d), (g), (j), (m), and (p), objective vectors of some solutions in the final population of the six PBEMO algorithms are near or in the ROI. However, the diversity of the final population in the ROI is poor for R-NSGA-II, r-NSGA-II, R-MEAD2, and MOEA/D-NUMS. This is because none of them maintains the best-so-far non-dominated solutions. Although PBEA and g-NSGA-II obtain the objective vectors that cover the ROI in the objective space, they do not fit in the ROI. Here, g-NSGA-II aims to approximate an ROI different from equation (1) [48].

Results of UA-IDDS. As shown in Figures 3(b), (e), (h), (k), (n), and (q), objective vectors of the solution subset found by applying the IDSS method to the UA cover the ROI. However, their distributions are too wide. Intuitively, PBEMO algorithms are likely to generate solutions only near the ROI in the objective space. In contrast, our results show that the six PBEMO algorithms can generate non-dominated solutions far from the ROI. This may be because the six PBEMO algorithms do not explicitly use a mating restriction.

Results of UA-PP. Figures 3(c), (f), (i), (l), (o), and (r) are similar to each other. The objective vectors in the solution subsets obtained by applying the proposed method to the UA are densely distributed in the ROI. In contrast to the above discussed results in the two cases, the objective vectors in the solution subsets appear to fit the ROI. We observed similar results on the DTLZ1 and DTLZ3 problems in Figures S.1 and S.2, where some PBEMO algorithms fail to approximate the ROI of the DTLZ4 problem.

5.1.2 Comparison using IGD⁺-C. Table 2 shows the average IGD⁺-C values of the three solution subsets on the DTLZ1–DTLZ4 problems over 31 runs. Table 2 shows the results of R-NSGA-II. Table S.1 shows the results of the other PBEMO algorithms. In Table 2, the best and second best data are highlighted by **dark gray** and **gray**, respectively. Let us consider the comparison of two solution sets \mathcal{X}_1 and \mathcal{X}_2 (e.g., POP and UA-PP) over 31 runs. The symbols in parentheses in Table 2 indicate that \mathcal{X}_1 performs significantly better (+) and significantly worse (–) than \mathcal{X}_2 in terms of IGD⁺-C according to the Wilcoxon rank-sum test with $p < 0.05$. The symbol \approx means that the two results are not significantly different. We compared 1) a pair of UA-DDS and POP, 2) a pair of UA-PP and POP, and 3) a pair of UA-PP and UA-IDDS. For example, as seen from Table 2, UA-IDDS performs significantly worse than POP on DTLZ1 with $m = 4$. UA-PP performs significantly better than POP on DTLZ1 with $m = 3$, but UA-PP and UA-IDDS are not significantly different.

As shown in Table 2, UA-IDDS outperforms POP in many cases. However, UA-IDDS performs significantly worse than POP on some

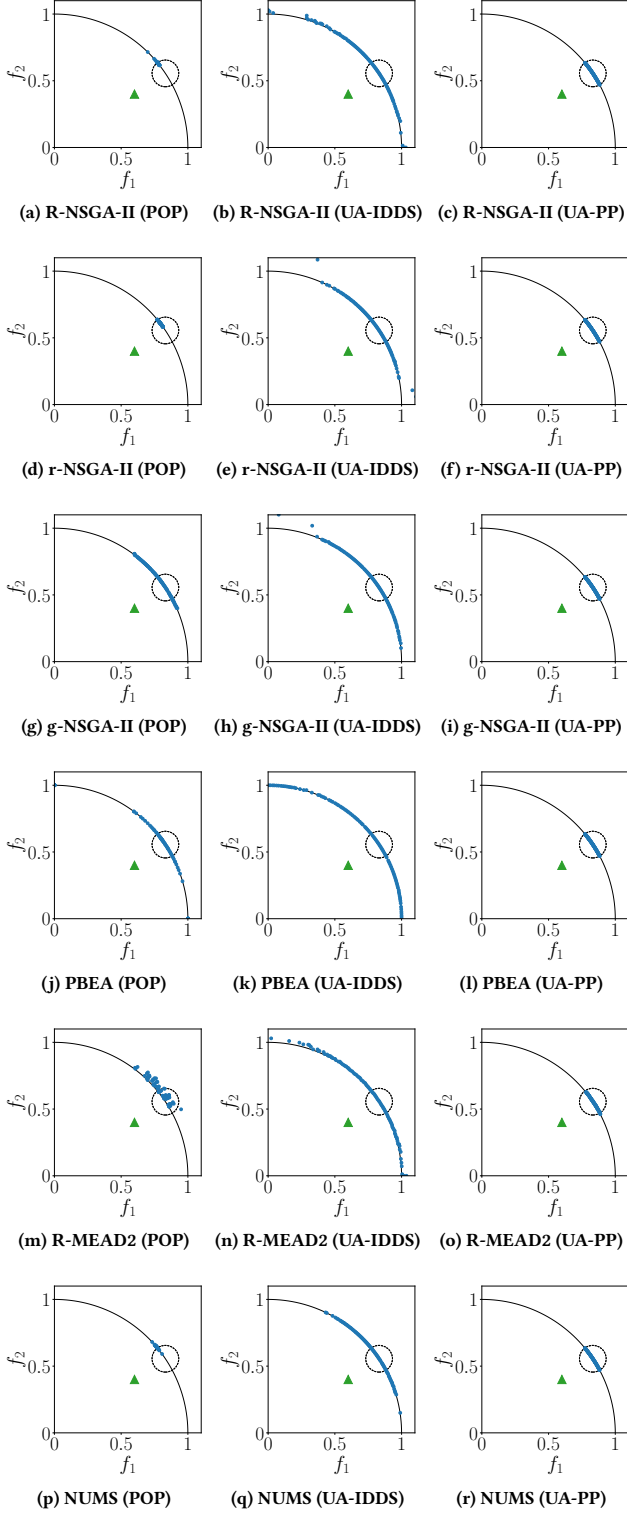


Figure 3: Distributions of the objective vectors of the solutions in the three solution sets on DTLZ2 with $m = 2$, where \blacktriangle is the reference point z . The dotted circle represents the true ROI. “NUMS” stands for MOEA/D-NUMS.

Table 2: Average IGD⁺-C values of the three solution subsets found by R-NSGA-II on the DTLZ1–DTLZ4 problems.

Problem	m	POP	UA-IDDS	UA-PP
DTLZ1	2	0.0236	0.0018 (+)	0.0012 (+, +)
	3	0.0334	0.0211 (+)	0.0220 (+, \approx)
	4	0.0562	0.0743 (-)	0.0442 (+, +)
	5	0.0933	0.0782 (+)	0.0558 (+, +)
	6	0.1131	0.0779 (+)	0.0695 (+, +)
	DTLZ2	2	0.0411	0.0016 (+)
3		0.1247	0.0276 (+)	0.0114 (+, +)
4		0.1986	0.0720 (+)	0.0339 (+, +)
5		0.2729	0.1162 (+)	0.0600 (+, +)
6		0.2840	0.1540 (+)	0.0853 (+, +)
DTLZ3		2	0.0345	0.0083 (+)
	3	0.1083	0.0460 (+)	0.0309 (+, +)
	4	0.1988	0.1736 (\approx)	0.0636 (+, +)
	5	0.2370	0.2169 (\approx)	0.1024 (+, +)
	6	0.8749	0.8287 (+)	0.7224 (+, +)
	DTLZ4	2	0.1014	0.0829 (\approx)
3		0.0838	0.0528 (+)	0.0375 (+, +)
4		0.1030	0.0741 (+)	0.0465 (+, +)
5		0.3757	0.1206 (+)	0.0759 (+, +)
6		0.3214	0.1144 (+)	0.0655 (+, +)

problems, e.g., DTLZ1 with $m = 4$. Similar results can be found in the results of the other five PBEMO algorithms as shown in Table S.1. This is because the objective vectors in UA-IDDS are widely distributed on the PF as shown in Figure 3.

In contrast, UA-PP performs significantly better than POP and UA-IDDS in most cases. UA-PP does not perform worse than POP. These results indicate the effectiveness of the UA in PBEMO and the importance of handling the DM’s preference information to postprocess the UA.

Answers to RQ1

Our results based on IGD⁺-C show that the performance of the six PBEMO algorithms can be significantly improved by using the UA. We observed that a better solution subset can be found by applying the proposed preference-based postprocessing method to the UA. This observation suggests the importance of incorporating the DM’s preference information in the postprocessing of the UA.

5.2 The impact of the population size

Based on the promising results of UA-PP in Section 5.1, this section and Section 5.3 evaluate the performance of PBEMO algorithms using the UA and the proposed postprocessing method. We performed 31 independent runs of the six PBEMO algorithms with the population sizes $\mu \in \{8, \dots, 500\}$ on the DTLZ1–DTLZ4 problems. Then, for each PBEMO algorithm, we calculated the average rankings of the population sizes $\mu \in \{8, \dots, 500\}$ by the Friedman test [21]. We used the CONTROL TEST package (<https://sci2s.ugr.es/sicidm>) to calculate the rankings based on the IGD⁺-C values. Below, we discuss the best-ranked population size for each number of objectives m and each budget of function evaluations.

Table 3 shows the best population size μ for $m \in \{2, 4, 6\}$ and $10^3, 5 \times 10^3, 10^4, 3 \times 10^4, 5 \times 10^4$ function evaluations on all of the

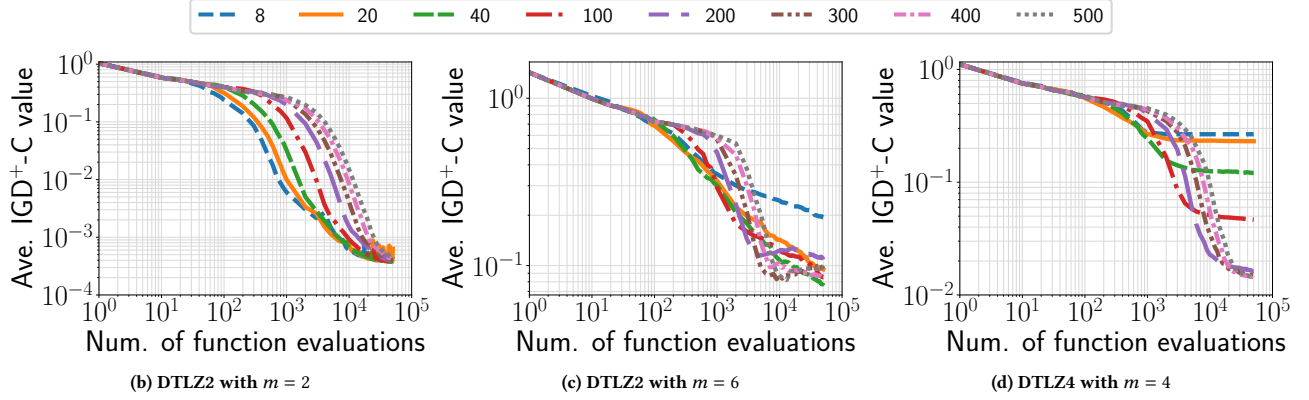


Figure 4: Average IGD⁺-C values of R-NSGA-II with different population sizes on three problems.

Table 3: The best population size μ for each number of function evaluations and $m \in \{2, 4, 6\}$ on the DTLZ1–DTLZ4 problems.

(a) $m = 2$					
PBEMO	1K FEs	5K FEs	10K FEs	30K FEs	50K FEs
R-NSGA-II	8	20	8	8	200
r-NSGA-II	20	20	20	40	40
g-NSGA-II	20	40	40	200	100
PBEA	20	40	8	100	200
R-MEAD2	8	8	8	20	20
MOEA/D-NUMS	8	8	8	20	20

(b) $m = 4$					
PBEMO	1K FEs	5K FEs	10K FEs	30K FEs	50K FEs
R-NSGA-II	8	40	20	20	20
r-NSGA-II	40	40	40	40	40
g-NSGA-II	40	100	200	400	400
PBEA	20	100	40	100	200
R-MEAD2	20	100	100	100	20
MOEA/D-NUMS	8	20	20	20	20

(c) $m = 6$					
PBEMO	1K FEs	5K FEs	10K FEs	30K FEs	50K FEs
R-NSGA-II	20	40	100	40	100
r-NSGA-II	40	40	100	100	100
g-NSGA-II	8	8	300	8	8
PBEA	20	40	100	300	300
R-MEAD2	8	100	200	20	40
MOEA/D-NUMS	20	40	40	20	20

DTLZ1–DTLZ4 problems. As seen from Table 3, $\mu = 500$ is not the best for any case. Table S.2 also shows the rankings of the eight μ values. As shown in Table S.2, $\mu = 500$ is the worst in most cases. Although some previous studies used a relatively large population size as shown in Table 1, this result suggests that a smaller population size than commonly used is effective for the PBEMO algorithms. Since we used the UA, the six PBEMO algorithms do not need to maintain good solutions for decision-making. This may be one of

the reasons why the six PBEMO algorithms do not require a large population size in this study.

As shown in Table 3(a), the best population size depends on the available budget of function evaluations. For example, $\mu = 8$ and $\mu = 200$ are the best for 10^3 and 5×10^4 function evaluations for R-NSGA-II. This property is more pronounced in the results of PBEA for many objectives. For example, as shown in the results of PBEA in Table 3(c), $\mu = 20$ and $\mu = 300$ perform the best for 10^3 and 5×10^4 function evaluations for $m = 6$. These results are consistent with the conclusions of the previous studies that investigated the influence of the population size on EMO algorithms (e.g., [10, 22, 26, 46]).

In contrast, we observed unexpected results for some PBEMO algorithms. For example, as shown in Table 3(c), $\mu = 8$ is suitable for R-MEAD2 for $m = 6$ and 10^3 function evaluations. For 10^4 function evaluations, $\mu = 200$ is the best for R-MEAD2. However, $\mu = 20$ and 40 are suitable for R-MEAD2 again for 3×10^4 and 5×10^4 function evaluations, respectively.

Below, we discuss the results on each test problem. Figure 4 shows the average IGD⁺-C values of R-NSGA-II with different population sizes on DTLZ2 with $m \in \{2, 6\}$ and DTLZ4 with $m = 4$. Figures S.4–S.9 show the results of the six PBEMO algorithms on all test problems. We do not discuss Figures S.4–S.9 due to the paper length limitation, but their results are similar to Figure 4.

As shown in Figure 4(a), R-NSGA-II with the smallest population size ($\mu = 8$) performs the best on DTLZ2 with $m = 2$ for a small budget of function evaluations. However, R-NSGA-II with $\mu = 8$ performs poorly as the number of function evaluations increases. As shown in Figure 4(b), this observation is more pronounced for many objectives. As seen Figure 4(b), the average IGD⁺-C values of R-NSGA-II with some μ values do not decrease monotonically as the number of function evaluations increases. This may be one of the reasons why R-NSGA-II with a relatively large population size (e.g., $\mu \in \{200, 300\}$) works well for 10^4 function evaluations, as discussed above. A monotonic decrease in the IGD⁺-C value may be achieved by using an indicator-based subset selection method [3] instead of the IDDS method. However, indicator-based subset selection methods generally require a higher computational cost than distance-based subset selection methods (e.g., the IDDS method).

A further investigation is another future work. As shown in Figure 4(c), R-NSGA-II with a small population size performs poorly on DTLZ4 with $m = 4$ as the search progresses. This observation suggests that PBEMO algorithms require a large population size on problems with a biased density of solutions.

Answers to RQ2

Our results show that a smaller population size than commonly used is effective for the six PBEMO algorithms for a small budget of function evaluations even for many objectives. We observed that the PBEMO algorithms require a large population size as the search progresses. However, our results suggest that a general rule of thumb “use a large population size on many-objective optimization problems with a large budget of function evaluations” may not be very helpful in determining the population size in PBEMO. Note that, of course, the best population size also depends on the type of PBEMO algorithm.

5.3 How the size of the ROI affects the best population size

In Sections 5.1 and 5.2, we set the radius of the ROI r to 0.1. Little is also known about the influence of the size of the ROI on the performance of PBEMO algorithms. Intuitively, PBEMO algorithms require a large-sized population to cover a large subregion of the PF. Thus, it is likely that the best population size depends on r .

Table 4 shows the best population size μ of R-NSGA-II on the DTLZ1–DTLZ4 problems with $r \in \{0.01, 0.05, 0.1, 0.2, 0.3\}$, where the results for $r = 0.1$ are the same as Table 3. Similar to Table 3, we determined the best population size according to the average rankings by the Friedman test. Tables S.3–S.7 show the results of the other PBEMO algorithms, but they are similar to Table 4.

As shown in Table 4, the best μ values for $r \in \{0.01, 0.05, 0.1\}$ are almost the same. In addition, a small population size is the best for a small budget of function evaluations. In contrast, as seen from the results for 5×10^4 function evaluations in Table 4, the best population size becomes large as r increases. However, we believe that $r = 0.3$ is too large as the size of the ROI. Recall that r is set to 0.1 in the example in Figure 1. If $r = 0.3$, the ROI in Figure 1 is almost the same as the PF. In preference-based multi-objective optimization, the DM is unlikely to want the solution set that covers the whole PF in the objective space (see Section 2.2).

Answers to RQ3

Our results show that the six PBEMO algorithms require a large-sized population when r , m , and a budget of function evaluations are large. However, the DM is unlikely to prefer a large r value. Only a limited budget of function evaluations is also available for some real-world problems [11]. Thus, we believe that a relatively small population size is a reasonable first choice in practice.

6 CONCLUSION

In this paper, we first proposed the preference-based method for postprocessing the UA in PBEMO. Unlike the existing postprocessing methods, the proposed method can handle the DM’s preference

Table 4: The best population size μ of R-NSGA-II on the DTLZ1–DTLZ4 problems with $r \in \{0.01, 0.05, 0.1, 0.2, 0.3\}$.

(a) $m = 2$					
r	1K FEs	5K FEs	10K FEs	30K FEs	50K FEs
0.01	8	20	8	20	20
0.05	8	20	8	20	20
0.1	8	20	8	8	200
0.2	20	20	8	100	200
0.3	20	40	8	100	300

(b) $m = 4$					
r	1K FEs	5K FEs	10K FEs	30K FEs	50K FEs
0.01	8	40	20	20	40
0.05	8	40	20	40	40
0.1	8	40	20	20	20
0.2	8	40	200	40	40
0.3	8	40	200	20	20

(c) $m = 6$					
r	1K FEs	5K FEs	10K FEs	30K FEs	50K FEs
0.01	20	40	300	40	40
0.05	20	40	300	40	40
0.1	20	40	100	40	100
0.2	20	100	100	200	300
0.3	20	100	100	200	300

information defined by the reference point z . Then, we investigated the effectiveness of the proposed preference-based postprocessing method on the DTLZ problems [20] with the number of objectives $m \in \{2, \dots, 6\}$. The results showed that the proposed method can obtain a better subset of the UA than the IDDS method [45] in most cases. The results also showed that the use of the UA and the proposed method can significantly improve the performance of the six PBEMO algorithms (R-NSGA-II [19], r-NSGA-II [41], g-NSGA-II [37], PBEA [49], R-MEAD2 [36], and MOEA/D-NUMS [28]). Our results revealed the difficulty in selecting a suitable population size in PBEMO algorithms. Although the best population size depends on some factors, our results suggest that a small population size (e.g., $\mu \in \{8, 20, 40\}$) for PBEMO algorithms is a good first choice, even for many objectives.

Although the benchmarking methodology has been investigated in the EMO literature (e.g., [9, 10, 25]), it has received little attention in the PBEMO literature. As reviewed in [1], benchmarking PBEMO algorithms is a challenging task. Our findings are helpful in establishing a systematic methodology for benchmarking PBEMO algorithms. This paper focused only on PBEMO algorithms using a single reference point. An investigation for multiple reference points is needed in future work. An analysis of PBEMO algorithms using other preference expressions (e.g., a value function) is another topic for future work.

ACKNOWLEDGMENTS

This work was supported by JSPS KAKENHI Grant Number 21K17824 and LEADER, MEXT, Japan.

REFERENCES

- [1] Bekir Afsar, Kaisa Miettinen, and Francisco Ruiz. 2021. Assessing the Performance of Interactive Multiobjective Optimization Methods: A Survey. *ACM Comput. Surv.* 54, 4 (2021), 85:1–85:27. <https://doi.org/10.1145/3448301>
- [2] Sunith Bandaru and Henrik Smedberg. 2019. A parameterless performance metric for reference-point based multi-objective evolutionary algorithms. In *Genetic and Evolutionary Computation Conference (GECCO)*. Anne Auger and Thomas Stützle (Eds.). ACM, 499–506. <https://doi.org/10.1145/3321707.3321757>
- [3] Matthieu Basseur, Bilel Derbel, Adrien Goëffon, and Arnaud Liefooghe. 2016. Experiments on Greedy and Local Search Heuristics for d -dimensional Hypervolume Subset Selection. In *Proceedings of the 2016 on Genetic and Evolutionary Computation Conference, Denver, CO, USA, July 20 - 24, 2016*, Tobias Friedrich, Frank Neumann, and Andrew M. Sutton (Eds.). ACM, 541–548. <https://doi.org/10.1145/2908812.2908949>
- [4] Slim Bechikh, Marouane Kessentini, Lamjed Ben Said, and Khaled Ghédira. 2015. Chapter Four - Preference Incorporation in Evolutionary Multiobjective Optimization: A Survey of the State-of-the-Art. *Adv. Comput.* 98 (2015), 141–207. <https://doi.org/10.1016/bs.adcom.2015.03.001>
- [5] Leonardo C. T. Bezerra, Manuel López-Ibáñez, and Thomas Stützle. 2019. Archiver effects on the performance of state-of-the-art multi- and many-objective evolutionary algorithms. In *Proceedings of the Genetic and Evolutionary Computation Conference, GECCO 2019, Prague, Czech Republic, July 13-17, 2019*, Anne Auger and Thomas Stützle (Eds.). ACM, 620–628. <https://doi.org/10.1145/3321707.3321789>
- [6] Julian Blank, Kalyanmoy Deb, Yashesh D. Dhebar, Sunith Bandaru, and Haitham Seada. 2021. Generating Well-Spaced Points on a Unit Simplex for Evolutionary Many-Objective Optimization. *IEEE Trans. Evol. Comput.* 25, 1 (2021), 48–60. <https://doi.org/10.1109/TEVC.2020.2992387>
- [7] Karl Bringmann, Sergio Cabello, and Michael T. M. Emmerich. 2017. Maximum Volume Subset Selection for Anchored Boxes. In *33rd International Symposium on Computational Geometry, SoCG 2017, July 4-7, 2017, Brisbane, Australia (LIPIcs, Vol. 77)*, Boris Aronov and Matthew J. Katz (Eds.). Schloss Dagstuhl - Leibniz-Zentrum für Informatik, 22:1–22:15. <https://doi.org/10.4230/LIPIcs.SocG.2017.22>
- [8] Karl Bringmann, Tobias Friedrich, and Patrick Klitzke. 2014. Generic Postprocessing via Subset Selection for Hypervolume and Epsilon-Indicator. In *Parallel Problem Solving from Nature - PPSN XIII - 13th International Conference, Ljubljana, Slovenia, September 13-17, 2014. Proceedings (Lecture Notes in Computer Science, Vol. 8672)*, Thomas Bartz-Beielstein, Jürgen Branke, Bogdan Filipic, and Jim Smith (Eds.). Springer, 518–527. https://doi.org/10.1007/978-3-319-10762-2_51
- [9] Dimo Brockhoff, Anne Auger, Nikolaus Hansen, and Tea Tusar. 2022. Using Well-Understood Single-Objective Functions in Multiobjective Black-Box Optimization Test Suites. *Evol. Comput.* 30, 2 (2022), 165–193. https://doi.org/10.1162/evco_a_00298
- [10] Dimo Brockhoff, Thanh-Do Tran, and Nikolaus Hansen. 2015. Benchmarking Numerical Multiobjective Optimizers Revisited. In *Proceedings of the Genetic and Evolutionary Computation Conference, GECCO 2015, Madrid, Spain, July 11-15, 2015*, Sara Silva and Anna Isabel Esparcia-Alcázar (Eds.). ACM, 639–646. <https://doi.org/10.1145/2739480.2754777>
- [11] Tinkle Chugh, Karthik Sindhya, Jussi Hakanen, and Kaisa Miettinen. 2019. A survey on handling computationally expensive multiobjective optimization problems with evolutionary algorithms. *Soft Comput.* 23, 9 (2019), 3137–3166. <https://doi.org/10.1007/s00500-017-2965-0>
- [12] Carlos A. Coello Coello. 2000. Handling preferences in evolutionary multiobjective optimization: a survey. In *Proceedings of the 2000 Congress on Evolutionary Computation, CEC 2000, La Jolla, CA, USA, July 16-19, 2000*, Ali M. S. Zalzala (Ed.). IEEE, 30–37. <https://doi.org/10.1109/CEC.2000.870272>
- [13] Carlos A. Coello Coello and Margarita Reyes Sierra. 2004. A Study of the Parallelization of a Coevolutionary Multi-objective Evolutionary Algorithm. In *Mexican International Conference on Artificial Intelligence (MICAI)*. 688–697. https://doi.org/10.1007/978-3-540-24694-7_71
- [14] David Corne, Joshua D. Knowles, and Martin J. Oates. 2000. The Pareto Envelope-Based Selection Algorithm for Multi-objective Optimisation. In *Parallel Problem Solving from Nature - PPSN VI, 6th International Conference, Paris, France, September 18-20, 2000. Proceedings (Lecture Notes in Computer Science, Vol. 1917)*, Marc Schoenauer, Kalyanmoy Deb, Günter Rudolph, Xin Yao, Evelyne Lutton, Juan Julián Merelo Guervós, and Hans-Paul Schwefel (Eds.). Springer, 839–848. https://doi.org/10.1007/3-540-45356-3_82
- [15] Kalyanmoy Deb. 2001. *Multi-objective optimization using evolutionary algorithms*. Wiley.
- [16] Kalyanmoy Deb, Samir Agrawal, Amrit Pratap, and T. Meyarivan. 2002. A fast and elitist multiobjective genetic algorithm: NSGA-II. *IEEE Trans. Evol. Comput.* 6, 2 (2002), 182–197. <https://doi.org/10.1109/4235.996017>
- [17] Kalyanmoy Deb and Himanshu Jain. 2014. An Evolutionary Many-Objective Optimization Algorithm Using Reference-Point-Based Nondominated Sorting Approach, Part I: Solving Problems With Box Constraints. *IEEE Trans. Evol. Comput.* 18, 4 (2014), 577–601. <https://doi.org/10.1109/TEVC.2013.2281535>
- [18] Kalyanmoy Deb, Manikant Mohan, and Shikhar Mishra. 2005. Evaluating the epsilon-Domination Based Multi-Objective Evolutionary Algorithm for a Quick Computation of Pareto-Optimal Solutions. *Evol. Comput.* 13, 4 (2005), 501–525. <https://doi.org/10.1162/106365605774666895>
- [19] Kalyanmoy Deb, J. Sundar, Udaya Bhaskara, and Shamik Chaudhuri. 2006. Reference Point Based Multi-Objective Optimization Using Evolutionary Algorithms. *Int. J. Comput. Intell.* 2, 3 (2006), 273–286.
- [20] Kalyanmoy Deb, Lothar Thiele, Marco Laumanns, and Eckart Zitzler. 2005. Scalable Test Problems for Evolutionary Multi-Objective Optimization. In *Evolutionary Multiobjective Optimization. Theoretical Advances and Applications*. Springer, 105–145.
- [21] Joaquín Derrac, Salvador García, Daniel Molina, and Francisco Herrera. 2011. A practical tutorial on the use of nonparametric statistical tests as a methodology for comparing evolutionary and swarm intelligence algorithms. *Swarm Evol. Comput.* 1, 1 (2011), 3–18. <https://doi.org/10.1016/j.swevo.2011.02.002>
- [22] Antoine S. D. Dymond, Schalk Kok, and P. Stephan Heyns. 2013. The sensitivity of multi-objective optimization algorithm performance to objective function evaluation budgets. In *Proceedings of the IEEE Congress on Evolutionary Computation, CEC 2013, Cancun, Mexico, June 20-23, 2013*. IEEE, 1868–1875. <https://doi.org/10.1109/CEC.2013.6557787>
- [23] Carlos M. Fonseca and Peter J. Fleming. 1993. Genetic Algorithms for Multiobjective Optimization: Formulation Discussion and Generalization. In *Proceedings of the 5th International Conference on Genetic Algorithms, Urbana-Champaign, IL, USA, June 1993*, Stephanie Forrest (Ed.). Morgan Kaufmann, 416–423.
- [24] Hisao Ishibuchi, Hiroyuki Masuda, Yuki Tanigaki, and Yusuke Nojima. 2015. Modified Distance Calculation in Generational Distance and Inverted Generational Distance. In *Evolutionary Multi-Criterion Optimization - 8th International Conference, EMO 2015, Guimarães, Portugal, March 29-April 1, 2015. Proceedings, Part II (Lecture Notes in Computer Science, Vol. 9019)*, António Gaspar-Cunha, Carlos Henggeler Antunes, and Carlos A. Coello Coello (Eds.). Springer, 110–125. https://doi.org/10.1007/978-3-319-15892-1_8
- [25] Hisao Ishibuchi, Lie Meng Pang, and Ke Shang. 2022. Difficulties in Fair Performance Comparison of Multi-Objective Evolutionary Algorithms [Research Frontier]. *IEEE Comput. Intell. Mag.* 17, 1 (2022), 86–101. <https://doi.org/10.1109/MCI.2021.3129961>
- [26] Hisao Ishibuchi, Yu Setoguchi, Hiroyuki Masuda, and Yusuke Nojima. 2016. How to compare many-objective algorithms under different settings of population and archive sizes. In *IEEE Congress on Evolutionary Computation, CEC 2016, Vancouver, BC, Canada, July 24-29, 2016*. IEEE, 1149–1156. <https://doi.org/10.1109/CEC.2016.7743917>
- [27] Andrzej Jaskiewicz and Thibaut Lust. 2018. ND-Tree-Based Update: A Fast Algorithm for the Dynamic Nondominance Problem. *IEEE Trans. Evol. Comput.* 22, 5 (2018), 778–791. <https://doi.org/10.1109/TEVC.2018.2799684>
- [28] Ke Li, Renzhi Chen, Geyong Min, and Xin Yao. 2018. Integration of Preferences in Decomposition Multiobjective Optimization. *IEEE Trans. Cybern.* 48, 12 (2018), 3359–3370. <https://doi.org/10.1109/TCYB.2018.2859363>
- [29] Ke Li, Kalyanmoy Deb, and Xin Yao. 2018. R-Metric: Evaluating the Performance of Preference-Based Evolutionary Multiobjective Optimization Using Reference Points. *IEEE Trans. Evol. Comput.* 22, 6 (2018), 821–835. <https://doi.org/10.1109/TEVC.2017.2737781>
- [30] Ke Li, Minhui Liao, Kalyanmoy Deb, Geyong Min, and Xin Yao. 2020. Does Preference Always Help? A Holistic Study on Preference-Based Evolutionary Multiobjective Optimization Using Reference Points. *IEEE Trans. Evol. Comput.* 24, 6 (2020), 1078–1096. <https://doi.org/10.1109/TEVC.2020.2987559>
- [31] Miqing Li and Xin Yao. 2019. Quality Evaluation of Solution Sets in Multiobjective Optimisation: A Survey. *ACM Comput. Surv.* 52, 2 (2019), 26:1–26:38. <https://doi.org/10.1145/3300148>
- [32] Manuel López-Ibáñez, Joshua D. Knowles, and Marco Laumanns. 2011. On Sequential Online Archiving of Objective Vectors. In *Evolutionary Multi-Criterion Optimization - 6th International Conference, EMO 2011, Ouro Preto, Brazil, April 5-8, 2011. Proceedings (Lecture Notes in Computer Science, Vol. 6576)*, Ricardo H. C. Takahashi, Kalyanmoy Deb, Elizabeth F. Wanner, and Salvatore Greco (Eds.). Springer, 46–60. https://doi.org/10.1007/978-3-642-19893-9_4
- [33] Kaisa Miettinen. 1998. *Nonlinear Multiobjective Optimization*. Springer.
- [34] Kaisa Miettinen and Marko M. Mäkelä. 2002. On scalarizing functions in multi-objective optimization. *OR Spectr.* 24, 2 (2002), 193–213. <https://doi.org/10.1007/s00291-001-0092-9>
- [35] Asad Mohammadi, Mohammad Nabi Omidvar, and Xiaodong Li. 2013. A new performance metric for user-preference based multi-objective evolutionary algorithms. In *IEEE Congress on Evolutionary Computation (CEC)*. IEEE, 2825–2832. <https://doi.org/10.1109/CEC.2013.6557912>
- [36] Asad Mohammadi, Mohammad Nabi Omidvar, Xiaodong Li, and Kalyanmoy Deb. 2014. Integrating user preferences and decomposition methods for many-objective optimization. In *IEEE Congress on Evolutionary Computation (CEC)*. IEEE, 421–428. <https://doi.org/10.1109/CEC.2014.6900595>
- [37] Julián Molina, Luis V. Santana-Quintero, Alfredo García Hernández-Díaz, Carlos A. Coello Coello, and Rafael Caballero. 2009. g-dominance: Reference point based dominance for multiobjective metaheuristics. *Eur. J. Oper. Res.* 197, 2 (2009), 685–692. <https://doi.org/10.1016/j.ejor.2008.07.015>

- [38] Robin C. Purshouse, Kalyanmoy Deb, Maszatul M. Mansor, Sanaz Mostaghim, and Rui Wang. 2014. A review of hybrid evolutionary multiple criteria decision making methods. In *IEEE Congress on Evolutionary Computation (CEC)*. IEEE, 1147–1154. <https://doi.org/10.1109/CEC.2014.6900368>
- [39] Andreea Radulescu, Manuel López-Ibáñez, and Thomas Stützle. 2013. Automatically Improving the Anytime Behaviour of Multiobjective Evolutionary Algorithms. In *Evolutionary Multi-Criterion Optimization - 7th International Conference, EMO 2013, Sheffield, UK, March 19-22, 2013. Proceedings (Lecture Notes in Computer Science, Vol. 7811)*, Robin C. Purshouse, Peter J. Fleming, Carlos M. Fonseca, Salvatore Greco, and Jane Shaw (Eds.). Springer, 825–840. https://doi.org/10.1007/978-3-642-37140-0_61
- [40] Ana Belen Ruiz, Rubén Saborido, and Mariano Luque. 2015. A preference-based evolutionary algorithm for multiobjective optimization: the weighting achievement scalarizing function genetic algorithm. *J. Glob. Optim.* 62, 1 (2015), 101–129. <https://doi.org/10.1007/s10898-014-0214-y>
- [41] Lamjed Ben Said, Slim Bechikh, and Khaled Ghédira. 2010. The r-Dominance: A New Dominance Relation for Interactive Evolutionary Multicriteria Decision Making. *IEEE Trans. Evol. Comput.* 14, 5 (2010), 801–818. <https://doi.org/10.1109/TEVC.2010.2041060>
- [42] Serpil Sayin. 2000. Measuring the quality of discrete representations of efficient sets in multiple objective mathematical programming. *Math. Program.* 87, 3 (2000), 543–560. <https://doi.org/10.1007/s101070050011>
- [43] Oliver Schütze, Xavier Esquivel, Adriana Lara, and Carlos A. Coello Coello. 2012. Using the Averaged Hausdorff Distance as a Performance Measure in Evolutionary Multiobjective Optimization. *IEEE Trans. Evol. Comput.* 16, 4 (2012), 504–522. <https://doi.org/10.1109/TEVC.2011.2161872>
- [44] Ke Shang, Hisao Ishibuchi, and Weiyu Chen. 2021. Greedy approximated hypervolume subset selection for many-objective optimization. In *GECCO '21: Genetic and Evolutionary Computation Conference, Lille, France, July 10-14, 2021*, Francisco Chicano and Krzysztof Krawiec (Eds.). ACM, 448–456. <https://doi.org/10.1145/3449639.3459390>
- [45] Ke Shang, Hisao Ishibuchi, and Yang Nan. 2021. Distance-based subset selection revisited. In *GECCO '21: Genetic and Evolutionary Computation Conference, Lille, France, July 10-14, 2021*, Francisco Chicano and Krzysztof Krawiec (Eds.). ACM, 439–447. <https://doi.org/10.1145/3449639.3459391>
- [46] Ryoji Tanabe and Hisao Ishibuchi. 2018. An analysis of control parameters of MOEA/D under two different optimization scenarios. *Appl. Soft Comput.* 70 (2018), 22–40. <https://doi.org/10.1016/j.asoc.2018.05.014>
- [47] Ryoji Tanabe, Hisao Ishibuchi, and Akira Oyama. 2017. Benchmarking Multi- and Many-Objective Evolutionary Algorithms Under Two Optimization Scenarios. *IEEE Access* 5 (2017), 19597–19619. <https://doi.org/10.1109/ACCESS.2017.2751071>
- [48] Ryoji Tanabe and Ke Li. 2023. Quality Indicators for Preference-based Evolutionary Multi-objective Optimization Using a Reference Point: A Review and Analysis. *CoRR abs/2301.12148* (2023). <https://doi.org/10.48550/arXiv.2301.12148> arXiv:2301.12148
- [49] Lothar Thiele, Kaisa Miettinen, Pekka J. Korhonen, and Julián Molina Luque. 2009. A Preference-Based Evolutionary Algorithm for Multi-Objective Optimization. *Evol. Comput.* 17, 3 (2009), 411–436. <https://doi.org/10.1162/evco.2009.17.3.411>
- [50] Andrzej P. Wierzbicki. 1980. The use of reference objectives in multiobjective optimization. In *Multiple Criteria Decision Making Theory and Application*. Springer, 468–486. https://doi.org/10.1007/978-3-642-48782-8_32
- [51] Qingfu Zhang and Hui Li. 2007. MOEA/D: A Multiobjective Evolutionary Algorithm Based on Decomposition. *IEEE Trans. Evol. Comput.* 11, 6 (2007), 712–731. <https://doi.org/10.1109/TEVC.2007.892759>
- [52] Eckart Zitzler and Simon Künzli. 2004. Indicator-Based Selection in Multiobjective Search. In *Parallel Problem Solving from Nature (PPSN)*. 832–842. https://doi.org/10.1007/978-3-540-30217-9_84
- [53] Eckart Zitzler, Marco Laumanns, and Lothar Thiele. 2001. *SPEA2: Improving the Strength Pareto Evolutionary Algorithm*. Technical Report 103. Swiss Federal Institute of Technology (ETHZ).
- [54] Eckart Zitzler and Lothar Thiele. 1998. Multiobjective Optimization Using Evolutionary Algorithms - A Comparative Case Study. In *Parallel Problem Solving from Nature (PPSN)*. Springer, 292–304. <https://doi.org/10.1007/BFb0056872>
- [55] Eckart Zitzler, Lothar Thiele, Marco Laumanns, Carlos M. Fonseca, and Viviane Grunert da Fonseca. 2003. Performance assessment of multiobjective optimizers: an analysis and review. *IEEE Trans. Evol. Comput.* 7, 2 (2003), 117–132. <https://doi.org/10.1109/TEVC.2003.810758>

Supplement

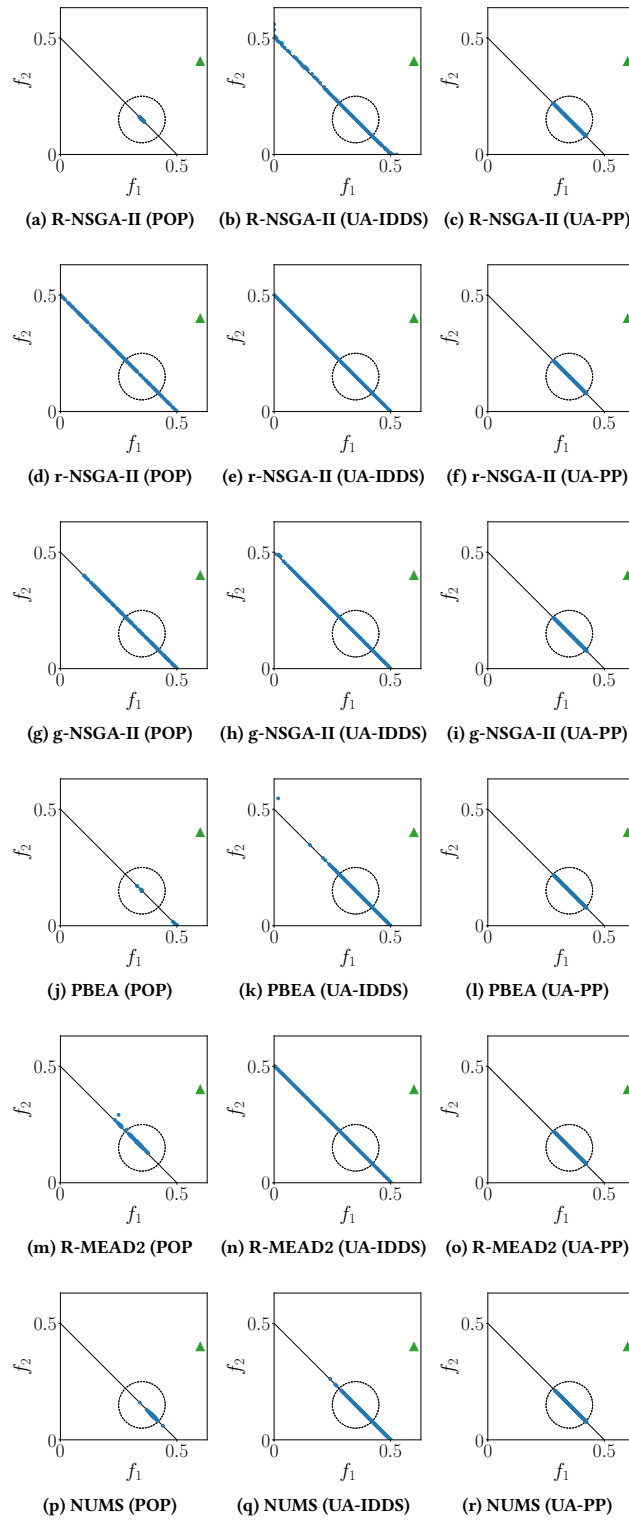


Figure S.1: Distributions of the objective vectors of the solutions in the three solution sets on DTLZ1 with $m = 2$, where \blacktriangle is the reference point z . The dotted circle represents the true ROI. “NUMS” stands for MOEA/D-NUMS.

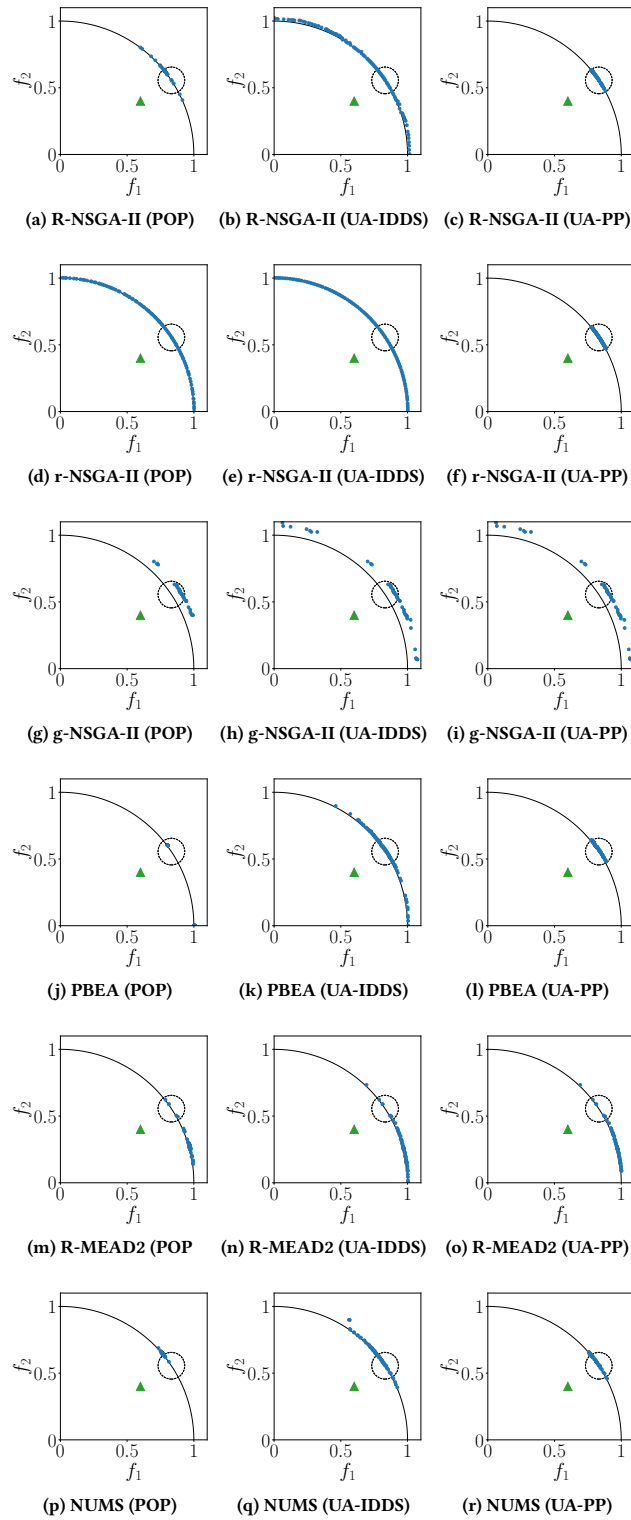


Figure S.2: Distributions of the objective vectors of the solutions in the three solution sets on DTLZ3 with $m = 2$, where \blacktriangle is the reference point z . The dotted circle represents the true ROI. “NUMS” stands for MOEA/D-NUMS.

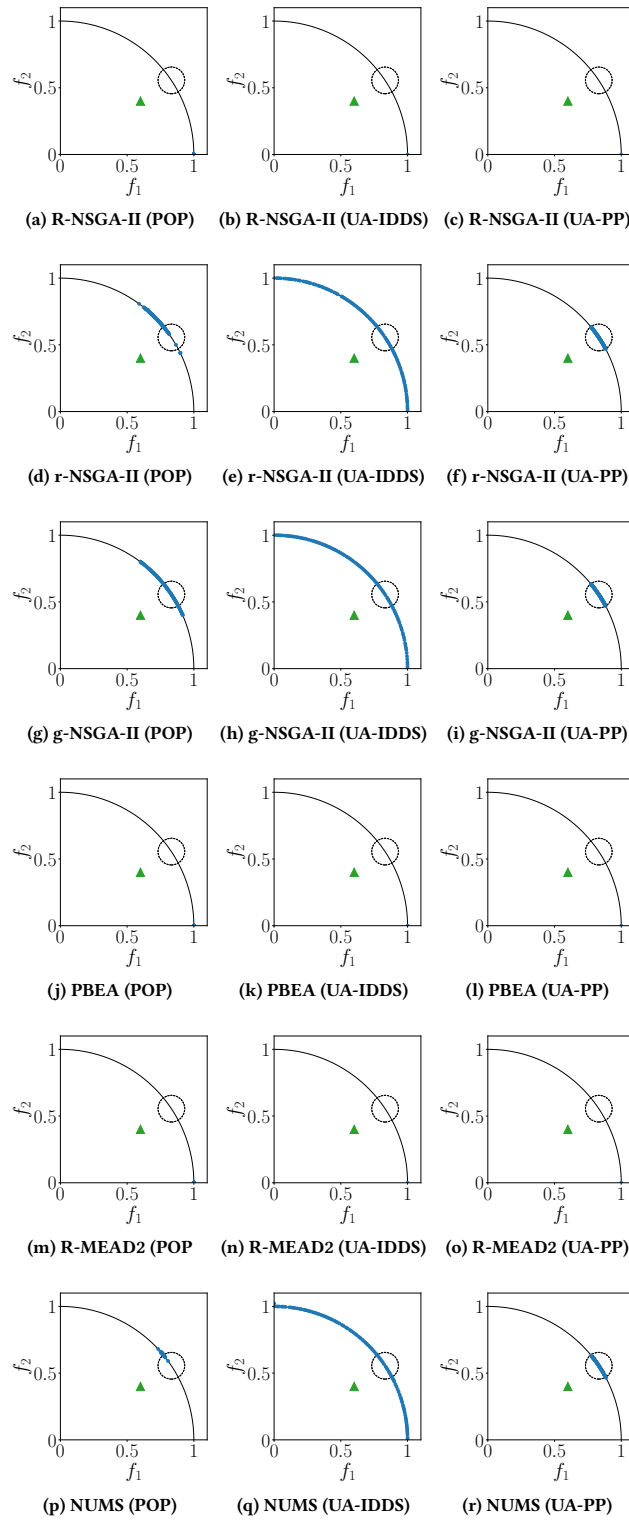


Figure S.3: Distributions of the objective vectors of the solutions in the three solution sets on DTLZ4 with $m = 2$, where \blacktriangle is the reference point z . The dotted circle represents the true ROI. “NUMS” stands for MOEA/D-NUMS.

Table S.1: Average IGD⁺-C values of the three solution subsets found by r-NSGA-II, g-NSGA-II, PBEA, R-MEAD2, and MOEA/D-NUMS on the DTLZ1–DTLZ4 problems.

(a) r-NSGA-II					(b) g-NSGA-II				
Problem	m	POP	UA-IDS	UA-PP	Problem	m	POP	UA-IDS	UA-PP
DTLZ1	2	0.0018	0.0015 (+)	0.0007 (+, +)	DTLZ1	2	0.0267	0.0265 (≈)	0.0259 (+, +)
	3	0.0221	0.0152 (+)	0.0079 (+, +)		3	10.7277	3.7391 (+)	3.7306 (+, ≈)
	4	0.6009	0.4523 (≈)	0.4361 (≈, ≈)		4	77.7690	20.7678 (+)	15.7325 (+, +)
	5	2.5538	1.8340 (+)	1.2448 (+, +)		5	123.8328	50.6386 (+)	23.8382 (+, +)
	6	2.9928	3.0074 (≈)	1.3174 (+, +)		6	145.9085	74.0552 (+)	30.8597 (+, +)
DTLZ2	2	0.0312	0.0015 (+)	0.0004 (+, +)	DTLZ2	2	0.0013	0.0019 (−)	0.0004 (+, +)
	3	0.0979	0.0255 (+)	0.0085 (+, +)		3	0.0264	0.0332 (−)	0.0090 (+, +)
	4	0.1700	0.0618 (+)	0.0222 (+, +)		4	0.2756	0.1978 (+)	0.0999 (+, +)
	5	0.1569	0.0967 (+)	0.0306 (+, +)		5	1.1044	0.5408 (+)	0.3901 (+, +)
	6	0.2044	0.1223 (+)	0.0505 (+, +)		6	1.3364	0.7812 (+)	0.4915 (+, +)
DTLZ3	2	0.0076	0.0075 (≈)	0.0060 (+, +)	DTLZ3	2	5.4893	5.3352 (≈)	5.3352 (≈, ≈)
	3	0.0905	0.0861 (≈)	0.0713 (+, +)		3	30.6638	27.3401 (≈)	27.3305 (≈, ≈)
	4	5.7675	5.5092 (≈)	5.3614 (≈, ≈)		4	266.2339	127.7268 (+)	119.3209 (+, ≈)
	5	11.0159	10.3284 (≈)	9.1448 (≈, ≈)		5	608.8715	352.6806 (+)	257.7681 (+, +)
	6	12.4904	11.4337 (≈)	9.7152 (≈, ≈)		6	851.7529	481.3857 (+)	340.8093 (+, +)
DTLZ4	2	0.0553	0.0454 (+)	0.0438 (+, +)	DTLZ4	2	1.3208	0.0347 (+)	0.0329 (+, +)
	3	0.0241	0.0280 (−)	0.0062 (+, +)		3	0.2915	0.0346 (+)	0.0116 (+, +)
	4	0.0306	0.0552 (−)	0.0153 (+, +)		4	0.0884	0.0851 (≈)	0.0344 (+, +)
	5	0.0657	0.0941 (−)	0.0278 (+, +)		5	0.4019	0.2268 (+)	0.1172 (+, +)
	6	0.1120	0.1155 (≈)	0.0367 (+, +)		6	0.7191	0.3082 (+)	0.2047 (+, +)

(c) PBEA					(d) R-MEAD2				
Problem	m	POP	UA-IDS	UA-PP	Problem	m	POP	UA-IDS	UA-PP
DTLZ1	2	0.0339	0.0009 (+)	0.0006 (+, +)	DTLZ1	2	0.0140	0.0072 (+)	0.0067 (+, ≈)
	3	0.0411	0.0121 (+)	0.0081 (+, +)		3	0.1785	0.1344 (≈)	0.1324 (≈, ≈)
	4	0.0609	0.0258 (+)	0.0175 (+, +)		4	0.2730	0.2247 (+)	0.2235 (+, ≈)
	5	0.0628	0.0385 (+)	0.0285 (+, +)		5	0.2630	0.2297 (≈)	0.2286 (+, ≈)
	6	0.0915	0.0647 (+)	0.0535 (+, +)		6	0.2874	0.2567 (≈)	0.2554 (≈, ≈)
DTLZ2	2	0.0012	0.0023 (−)	0.0003 (+, +)	DTLZ2	2	0.0112	0.0032 (+)	0.0019 (+, +)
	3	0.0420	0.0263 (+)	0.0053 (+, +)		3	0.0931	0.0352 (+)	0.0141 (+, +)
	4	0.0550	0.0590 (−)	0.0296 (+, +)		4	0.2894	0.1176 (+)	0.0948 (+, +)
	5	0.0799	0.1030 (−)	0.0527 (+, +)		5	0.3439	0.2084 (+)	0.1837 (+, ≈)
	6	0.1494	0.1536 (≈)	0.1412 (+, +)		6	0.4480	0.3216 (+)	0.3077 (+, ≈)
DTLZ3	2	0.0571	0.0061 (+)	0.0059 (+, ≈)	DTLZ3	2	0.1931	0.1437 (≈)	0.1439 (≈, ≈)
	3	0.1553	0.0804 (+)	0.0963 (+, ≈)		3	0.6909	0.6211 (+)	0.6211 (+, ≈)
	4	0.2022	0.1328 (+)	0.1664 (+, ≈)		4	0.8050	0.7381 (+)	0.7381 (+, ≈)
	5	0.2503	0.2114 (≈)	0.2389 (≈, ≈)		5	0.7892	0.7068 (+)	0.7093 (+, ≈)
	6	0.3300	0.2740 (+)	0.3157 (≈, −)		6	0.8368	0.7823 (+)	0.7824 (+, ≈)
DTLZ4	2	0.0768	0.0775 (−)	0.0763 (+, +)	DTLZ4	2	0.1639	0.1580 (≈)	0.1579 (≈, ≈)
	3	0.0580	0.0470 (+)	0.0281 (+, +)		3	0.1734	0.1711 (≈)	0.1710 (≈, ≈)
	4	0.0897	0.0886 (≈)	0.0660 (+, +)		4	0.2456	0.2404 (≈)	0.2401 (≈, ≈)
	5	0.1183	0.1309 (−)	0.0884 (+, +)		5	0.2958	0.2662 (+)	0.2629 (+, ≈)
	6	0.1506	0.1488 (≈)	0.1174 (+, +)		6	0.2598	0.2409 (+)	0.2443 (≈, ≈)

(e) MOEA/D-NUMS				
Problem	m	POP	UA-IDS	UA-PP
DTLZ1	2	0.0148	0.0007 (+)	0.0014 (+, −)
	3	0.0278	0.0092 (+)	0.0054 (+, +)
	4	0.0423	0.0263 (+)	0.0149 (+, +)
	5	0.0339	0.0341 (≈)	0.0231 (+, +)
	6	0.0378	0.0449 (−)	0.0311 (+, +)
DTLZ2	2	0.0452	0.0014 (+)	0.0004 (+, +)
	3	0.1464	0.0426 (+)	0.0345 (+, +)
	4	0.2161	0.1256 (+)	0.1012 (+, +)
	5	0.1696	0.1360 (+)	0.0965 (+, +)
	6	0.2392	0.2457 (−)	0.1780 (+, +)
DTLZ3	2	0.0834	0.0424 (+)	0.0426 (+, ≈)
	3	0.2056	0.1373 (+)	0.1405 (+, ≈)
	4	0.2958	0.2411 (+)	0.2257 (+, ≈)
	5	0.4276	0.4491 (≈)	0.3911 (+, +)
	6	0.7108	0.7999 (−)	0.6825 (≈, +)
DTLZ4	2	0.0453	0.0030 (+)	0.0007 (+, +)
	3	0.1476	0.0425 (+)	0.0430 (+, ≈)
	4	0.2308	0.0929 (+)	0.0831 (+, +)
	5	0.1802	0.1255 (+)	0.0926 (+, +)
	6	0.2639	0.2134 (+)	0.2046 (+, +)

Table S.2: The rankings of the eight μ values for each number of function evaluations and $m \in \{2, 4, 6\}$ on the DTLZ1–DTLZ4 problems (1st/2nd/3rd/4th/5th/6th/7th/8th).

(a) $m = 2$						
PBEMO	1K FEs	5K FEs	10K FEs	30K FEs	50K FEs	
R-NSGA-II	8/20/40/100/200/300/400/500	20/40/8/100/200/300/400/500	8/20/40/100/200/300/400/500	8/100/40/200/20/300/400/500	200/100/300/40/400/8/20/500	
r-NSGA-II	20/40/8/100/200/300/400/500	20/40/8/100/200/300/400/500	20/8/40/100/200/300/400/500	40/20/100/8/200/300/400/500	40/20/100/8/200/300/400/500	
g-NSGA-II	20/8/40/100/200/300/400/500	40/100/20/200/8/300/400/500	40/100/200/20/300/400/8/500	200/100/40/300/400/20/500/8	100/200/40/300/20/400/500/8	
PBEA	20/40/8/100/200/300/400/500	40/20/8/200/100/300/400/500	8/20/40/100/200/300/400/500	100/40/20/300/200/8/400/500	200/40/100/300/20/400/8/500	
R-MEAD2	8/20/40/100/200/300/400/500	8/20/40/100/200/300/400/500	8/20/40/100/200/300/400/500	20/40/100/8/200/300/400/500	20/40/100/200/300/8/400/500	
MOEA/D-NUMS	8/20/40/100/200/300/400/500	8/20/100/40/200/300/400/500	8/20/40/200/100/300/400/500	20/100/40/8/200/300/400/500	20/100/40/200/8/300/400/500	

(b) $m = 4$						
PBEMO	1K FEs	5K FEs	10K FEs	30K FEs	50K FEs	
R-NSGA-II	8/20/40/100/200/300/400/500	40/100/20/200/8/300/400/500	20/200/300/40/100/8/400/500	20/40/300/400/8/100/200/500	20/40/100/400/300/500/8/200	
r-NSGA-II	40/20/8/100/200/300/400/500	40/20/100/200/8/300/400/500	40/20/100/200/8/300/400/500	40/20/100/8/200/300/400/500	40/20/8/100/200/300/400/500	
g-NSGA-II	40/20/8/100/200/300/400/500	100/200/300/40/20/400/500/8	200/300/100/400/500/40/20/8	400/500/300/200/100/40/20/8	400/500/200/300/100/40/20/8	
PBEA	20/40/8/100/200/300/400/500	100/40/20/200/300/8/400/500	40/100/20/200/300/8/400/500	100/200/300/400/40/500/20/8	200/300/400/40/100/500/20/8	
R-MEAD2	20/8/40/100/300/200/400/500	100/20/200/8/40/300/400/500	100/200/8/20/300/40/400/500	100/20/8/200/400/40/300/500	20/8/100/300/500/40/200/400	
MOEA/D-NUMS	8/20/40/100/200/400/300/500	20/8/40/100/200/300/400/500	20/8/40/100/200/300/400/500	20/40/8/200/100/300/400/500	20/40/8/100/200/300/400/500	

(c) $m = 6$						
PBEMO	1K FEs	5K FEs	10K FEs	30K FEs	50K FEs	
R-NSGA-II	20/40/100/8/200/300/400/500	40/100/200/20/300/8/400/500	100/200/300/20/40/8/400/500	40/20/200/400/100/300/500/8	100/40/400/20/500/8/200/300	
r-NSGA-II	40/20/100/8/200/300/400/500	40/100/200/8/20/300/400/500	100/40/20/200/8/300/400/500	100/20/40/200/8/300/400/500	100/40/20/200/8/300/400/500	
g-NSGA-II	8/20/200/100/400/40/300/500	8/500/300/400/200/20/40/100	300/8/500/400/200/20/40/100	8/500/400/300/20/200/40/100	8/500/400/20/300/200/40/100	
PBEA	20/40/8/100/200/300/400/500	40/100/200/20/300/400/8/500	100/200/40/300/20/400/8/500	300/100/200/400/500/40/20/8	300/400/200/100/500/40/20/8	
R-MEAD2	8/40/20/100/200/300/400/500	100/200/8/20/40/300/400/500	200/300/8/20/100/400/40/500	20/200/40/100/400/500/300/8	40/20/100/200/400/500/8/300	
MOEA/D-NUMS	20/8/40/100/200/300/400/500	40/100/8/20/200/300/400/500	40/20/100/8/200/400/300/500	20/40/100/8/200/300/400/500	20/40/100/8/200/300/400/500	

Table S.3: The best population size μ of r-NSGA-II on the DTLZ1–DTLZ4 problems with $r \in \{0.01, 0.05, 0.1, 0.2, 0.3\}$.

(a) $m = 2$						
r	1K FEs	5K FEs	10K FEs	30K FEs	50K FEs	
0.01	20	20	8	100	40	
0.05	20	20	20	100	40	
0.1	20	20	20	40	40	
0.2	20	20	8	40	40	
0.3	20	20	8	40	40	

(b) $m = 4$						
r	1K FEs	5K FEs	10K FEs	30K FEs	50K FEs	
0.01	40	40	40	40	40	
0.05	40	40	40	40	40	
0.1	40	40	40	40	40	
0.2	20	40	40	40	40	
0.3	20	40	20	40	40	

(c) $m = 6$						
r	1K FEs	5K FEs	10K FEs	30K FEs	50K FEs	
0.01	40	40	40	100	100	
0.05	40	40	40	100	100	
0.1	40	40	100	100	100	
0.2	40	40	100	100	40	
0.3	40	40	40	40	40	

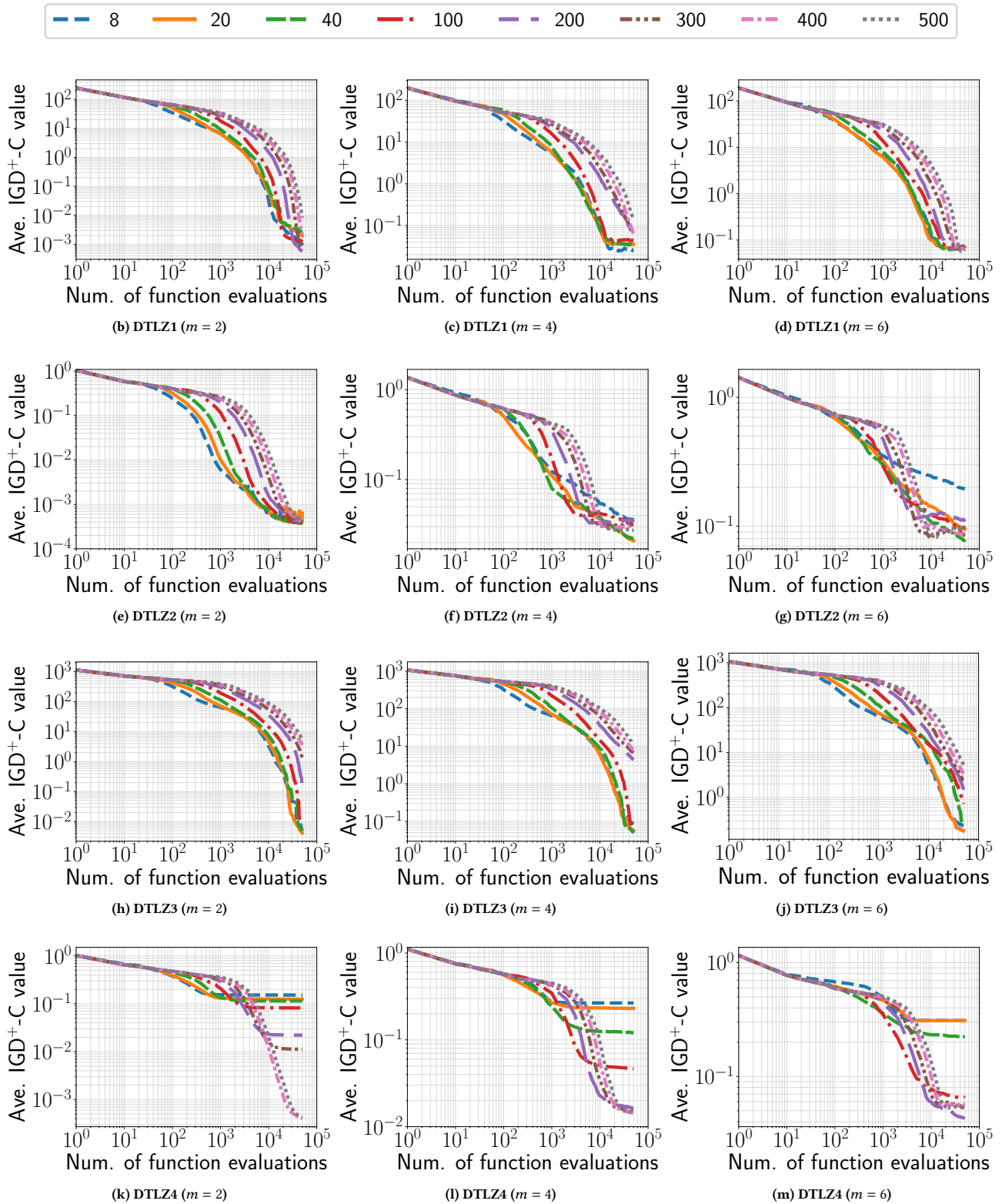


Figure S.4: Average IGD^{+-C} values of R-NSGA-II with different population sizes on the DTLZ1–DTLZ4 problems with $m \in \{2, 4, 6\}$.

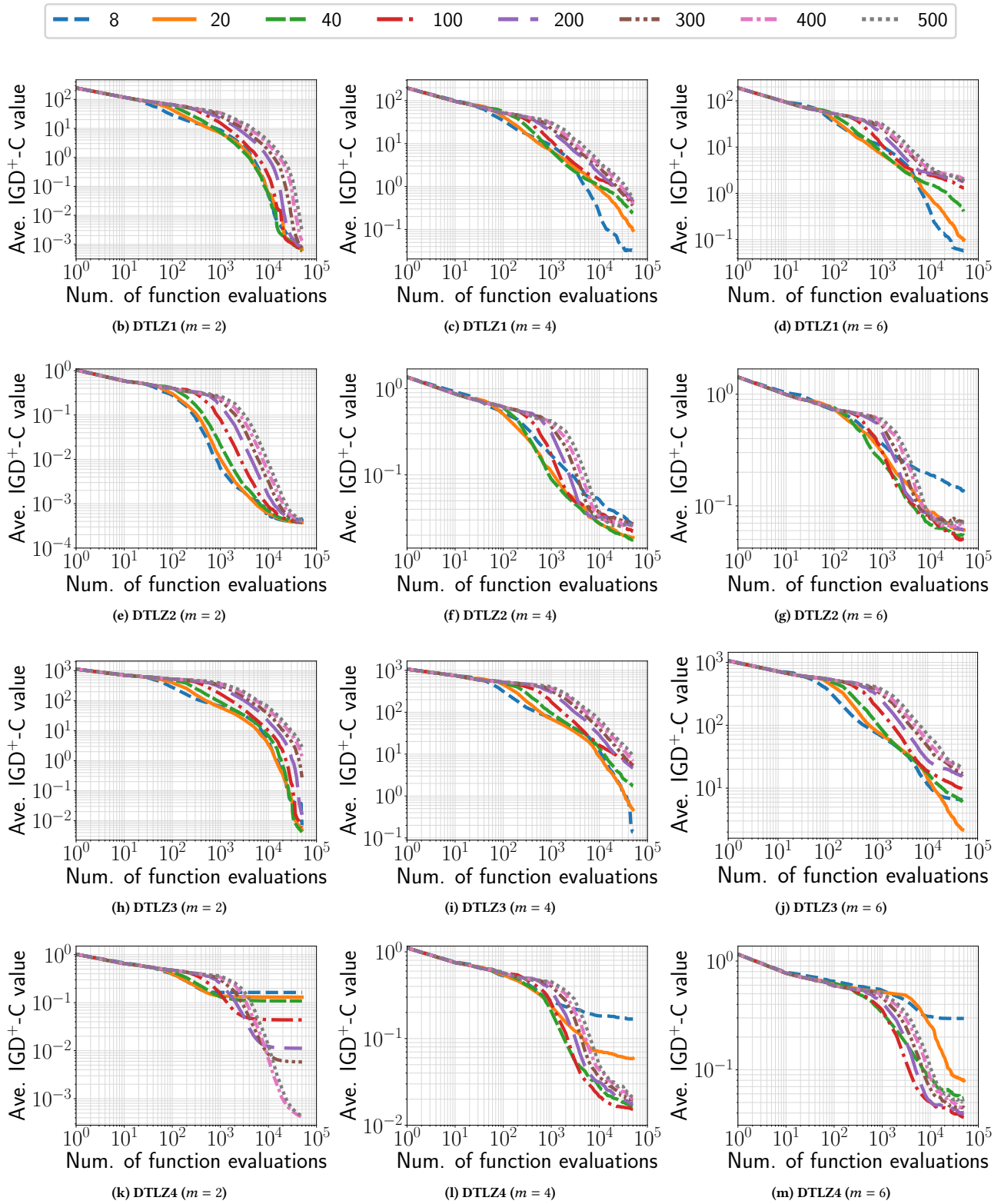


Figure S.5: Average IGD⁺⁻C values of r-NSGA-II with different population sizes on the DTLZ1–DTLZ4 problems with $m \in \{2, 4, 6\}$.

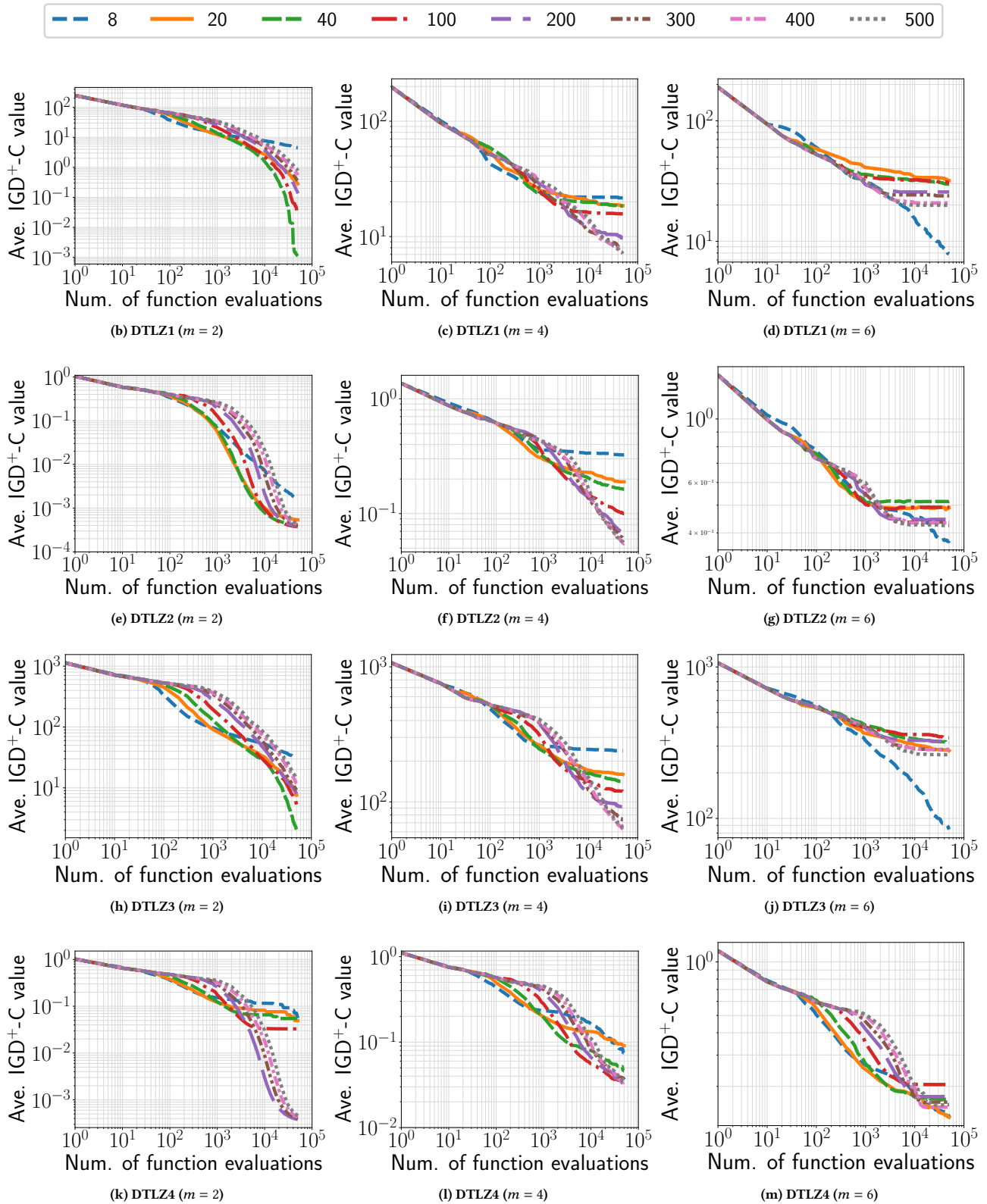


Figure S.6: Average IGD^{+-C} values of g-NSGA-II with different population sizes on the DTLZ1–DTLZ4 problems with $m \in \{2, 4, 6\}$.

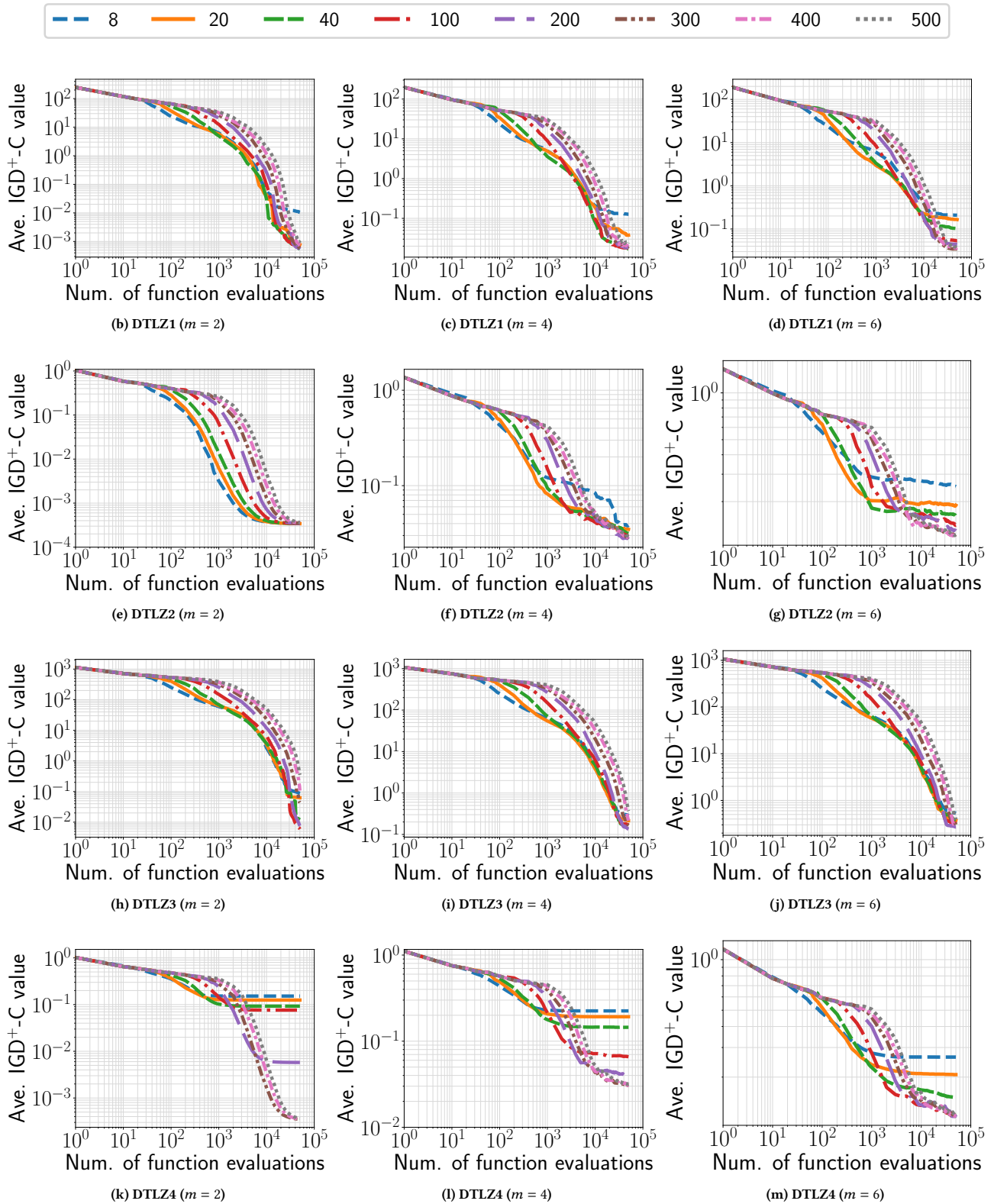


Figure S.7: Average IGD^{+-C} values of PBEA with different population sizes on the DTLZ1–DTLZ4 problems with $m \in \{2, 4, 6\}$.

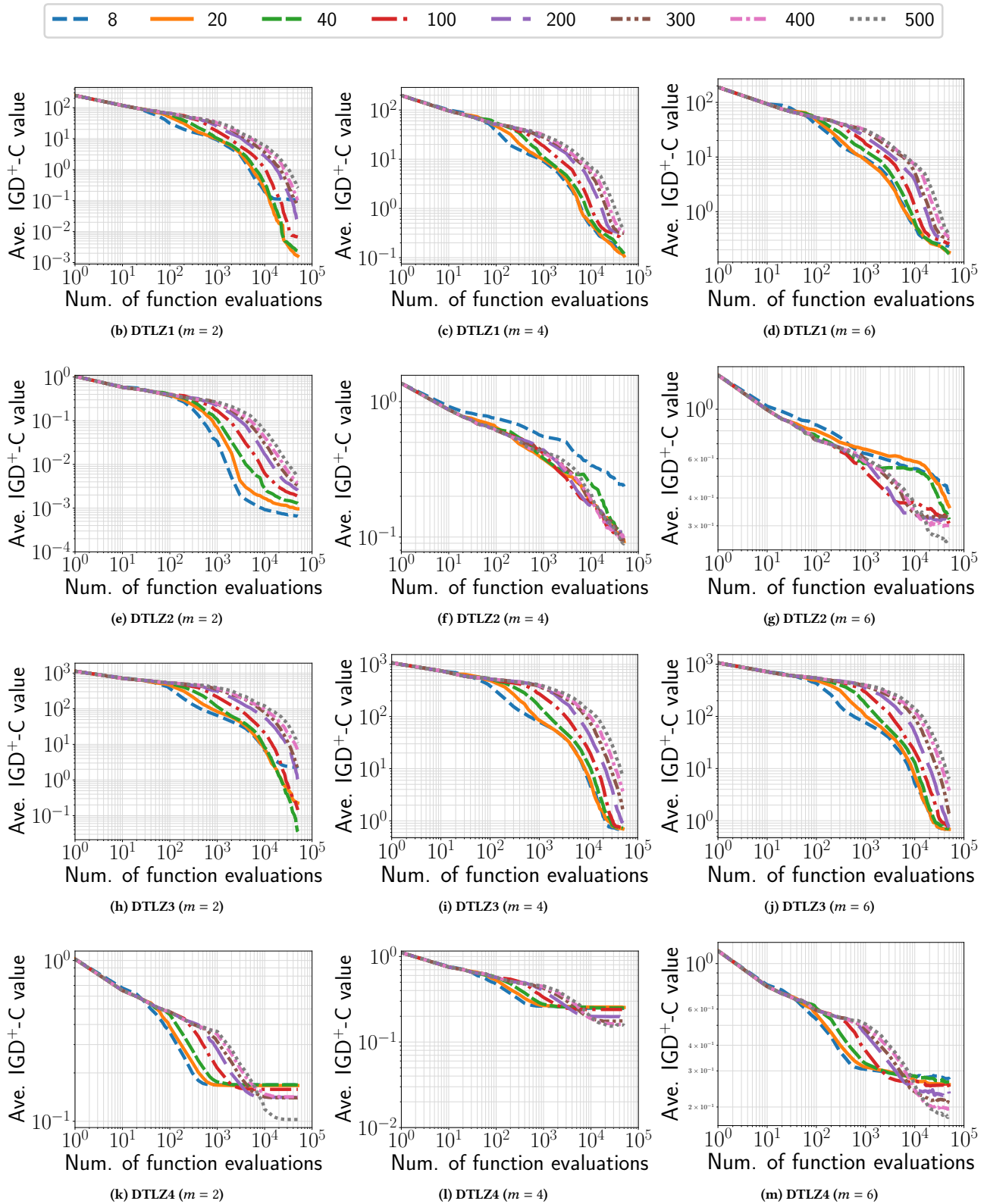


Figure S.8: Average IGD⁺⁻C values of R-MEAD2 with different population sizes on the DTLZ1–DTLZ4 problems with $m \in \{2, 4, 6\}$.

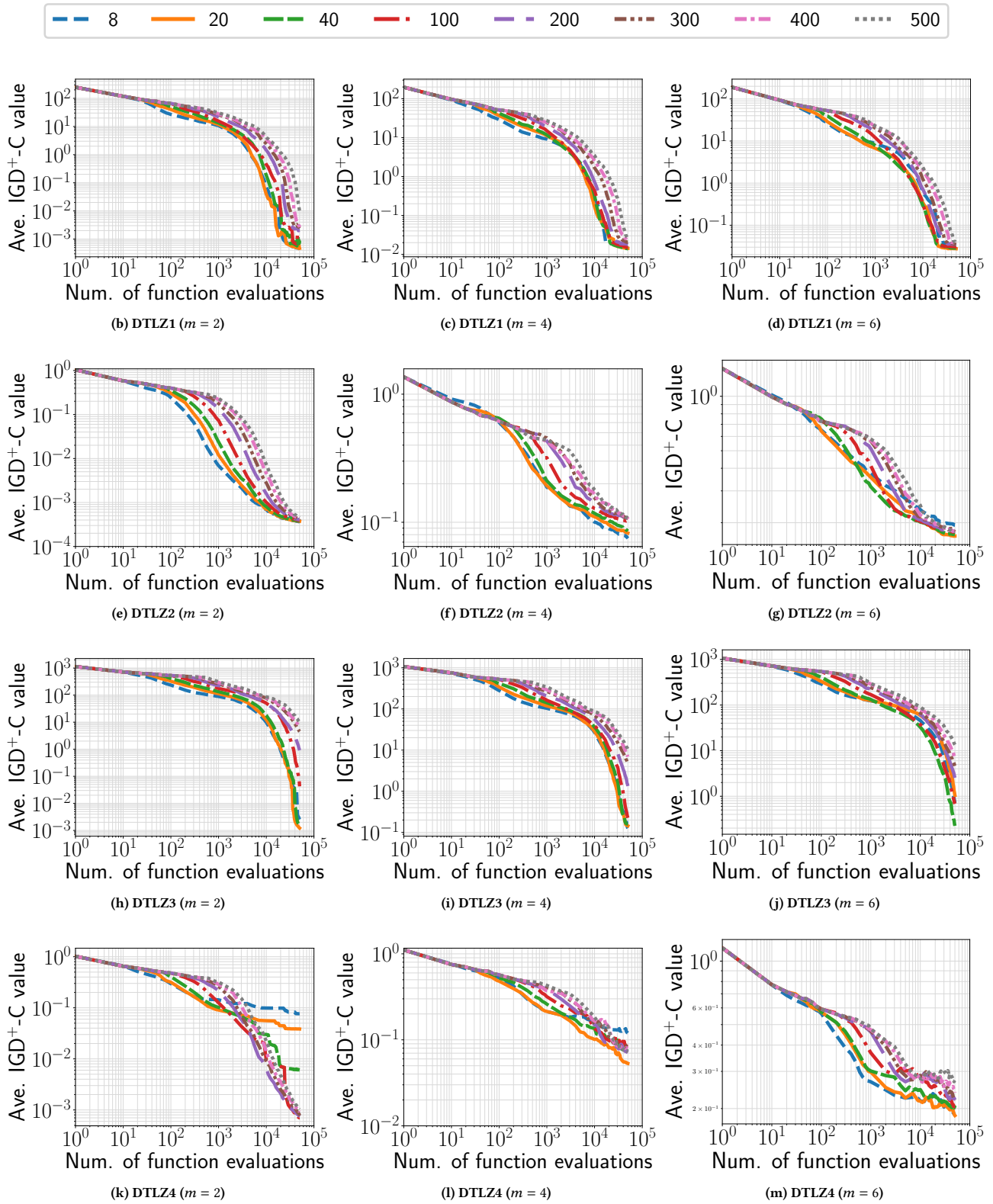


Figure S.9: Average IGD⁺⁻C values of MOEAD-NUMS with different population sizes on the DTLZ1-DTLZ4 problems with $m \in \{2, 4, 6\}$.

Table S.4: The best population size μ of g-NSGA-II on the DTLZ1–DTLZ4 problems with $r \in \{0.01, 0.05, 0.1, 0.2, 0.3\}$.

(a) $m = 2$					
r	1K FEs	5K FEs	10K FEs	30K FEs	50K FEs
0.01	20	40	40	200	100
0.05	20	40	40	200	100
0.1	20	40	40	200	100
0.2	20	40	40	40	100
0.3	20	40	40	200	100

(b) $m = 4$					
r	1K FEs	5K FEs	10K FEs	30K FEs	50K FEs
0.01	40	100	200	400	400
0.05	40	100	200	400	400
0.1	40	100	200	400	400
0.2	40	100	200	400	400
0.3	40	100	200	400	400

(c) $m = 6$					
r	1K FEs	5K FEs	10K FEs	30K FEs	50K FEs
0.01	8	8	300	8	8
0.05	8	8	300	8	8
0.1	8	8	300	8	8
0.2	8	8	8	8	8
0.3	8	8	8	8	8

Table S.5: The best population size μ of PBEA on the DTLZ1–DTLZ4 problems with $r \in \{0.01, 0.05, 0.1, 0.2, 0.3\}$.

(a) $m = 2$					
r	1K FEs	5K FEs	10K FEs	30K FEs	50K FEs
0.01	20	40	8	100	40
0.05	20	40	8	100	200
0.1	20	40	8	100	200
0.2	20	40	20	100	40
0.3	20	40	40	100	300

(b) $m = 4$					
r	1K FEs	5K FEs	10K FEs	30K FEs	50K FEs
0.01	20	100	40	200	200
0.05	20	100	40	200	200
0.1	20	100	40	100	200
0.2	20	100	40	200	200
0.3	20	100	40	200	300

(c) $m = 6$					
r	1K FEs	5K FEs	10K FEs	30K FEs	50K FEs
0.01	20	40	100	300	200
0.05	20	40	100	300	400
0.1	20	40	100	300	300
0.2	20	40	100	300	400
0.3	20	40	100	300	400

Table S.6: The best population size μ of R-MEAD2 on the DTLZ1–DTLZ4 problems with $r \in \{0.01, 0.05, 0.1, 0.2, 0.3\}$.

(a) $m = 2$					
r	1K FEs	5K FEs	10K FEs	30K FEs	50K FEs
0.01	8	8	8	20	20
0.05	8	8	8	20	20
0.1	8	8	8	20	20
0.2	8	8	8	20	20
0.3	8	8	8	20	20

(b) $m = 4$					
r	1K FEs	5K FEs	10K FEs	30K FEs	50K FEs
0.01	20	100	20	20	20
0.05	20	100	20	20	20
0.1	20	100	100	100	20
0.2	20	100	100	100	20
0.3	20	100	200	100	100

(c) $m = 6$					
r	1K FEs	5K FEs	10K FEs	30K FEs	50K FEs
0.01	8	100	200	20	40
0.05	8	100	200	20	40
0.1	8	100	200	20	40
0.2	8	100	200	20	40
0.3	8	100	300	20	20

Table S.7: The best population size μ of MOEA/D-NUMS on the DTLZ1–DTLZ4 problems with $r \in \{0.01, 0.05, 0.1, 0.2, 0.3\}$.

(a) $m = 2$					
r	1K FEs	5K FEs	10K FEs	30K FEs	50K FEs
0.01	8	8	8	100	20
0.05	8	8	8	20	40
0.1	8	8	8	20	20
0.2	8	20	20	20	20
0.3	8	8	20	8	20

(b) $m = 4$					
r	1K FEs	5K FEs	10K FEs	30K FEs	50K FEs
0.01	8	20	20	20	20
0.05	8	20	20	20	20
0.1	8	20	20	20	20
0.2	8	20	20	20	20
0.3	8	20	20	20	20

(c) $m = 6$					
r	1K FEs	5K FEs	10K FEs	30K FEs	50K FEs
0.01	20	40	40	20	20
0.05	20	40	40	20	20
0.1	20	40	40	20	20
0.2	8	40	40	20	20
0.3	8	40	40	20	20